HHS Public Access

Author manuscript

Cell Rep. Author manuscript; available in PMC 2021 June 22.

Published in final edited form as:

Cell Rep. 2021 May 18; 35(7): 109142. doi:10.1016/j.celrep.2021.109142.

Inhibitory affinity modulation of FcγRIIA ligand binding by glycosphingolipids by inside-out signaling

Koshu Okubo[1], **Michael D. Brenner**[2,6], **Xavier Cullere**[1,6], **Gurpanna Saggu**[1], **Myra L. Patchen**[3], **Nandita Bose**[4], **Saki Mihori**[1], **Zhou Yuan**[2], **Clifford A. Lowell**[5], **Cheng Zhu**[2], **Tanya N. Mayadas**[1,7,*]

[1]Department of Pathology, Brigham and Women's Hospital & Harvard Medical School, Boston, MA 02115, USA

[2]Institute for Bioengineering and Biosciences, Georgia Institute of Technology, Atlanta, GA 30332, USA

[3]Immuno Research, Inc., Eagan, MN 55121, USA

[4]Biothera Pharmaceuticals, Inc., Eagan, Minnesota, MN 55121, USA

[5]Department of Laboratory Medicine, University of California, San Francisco, CA 94143, USA

[6]These authors contributed equally

[7]Lead contact

SUMMARY

The interaction of the human FcγRIIA with immune complexes (ICs) promotes neutrophil activation and thus must be tightly controlled to avoid damage to healthy tissue. Here, we demonstrate that a fungal-derived soluble β-1,3/1,6-glucan binds to the glycosphingolipid long-chain lactosylceramide (LacCer) to reduce FcγRIIA-mediated recruitment to immobilized ICs under flow, a process requiring high-affinity FcγRIIA-immunoglobulin G (IgG) interactions. The inhibition requires Lyn phosphorylation of SHP-1 phosphatase and the FcγRIIA immunotyrosine-activating motif. β-glucan reduces the effective 2D affinity of FcγRIIA for IgG via Lyn and SHP-1 and, *in vivo*, inhibits FcγRIIA-mediated neutrophil recruitment to intravascular IgG deposited in the kidney glomeruli in a glycosphingolipid- and Lyn-dependent manner. In contrast, β-glucan did not affect FcγR functions that bypass FcγR affinity for IgG. In summary, we have identified a pathway for modulating the 2D affinity of FcγRIIA for ligand that relies on LacCer-Lyn-SHP-1-

*Correspondence: tmayadas@rics.bwh.harvard.edu.

AUTHOR CONTRIBUTIONS

K.O., M.D.B., X.C., G.S., Z.Y., and S.M. performed research and analyzed data. X.C. also contributed vital new reagents. M.L.P., N.B., and C.A.L. provided reagents and conceptual insights. C.Z. supervised the biophysical studies. T.N.M. conceptualized and designed and supervised the research. K.O. and T.N.M. wrote the manuscript, and M.D.B. and C.Z. wrote the biophysical studies. All authors edited the manuscript.

DECLARATION OF INTERESTS

M.L.P. owns stock/stock options in Biothera Pharmaceuticals, Inc. and is employed by Immuno Research, Inc. N.B. is employed by and own stock/stock options in Biothera Pharmaceuticals, Inc. The remaining authors have no conflicts of interest to disclose.

SUPPLEMENTAL INFORMATION

Supplemental information can be found online at https://doi.org/10.1016/j.celrep.2021.109142.

mediated inhibitory signaling triggered by β-glucan, a previously described activator of innate immunity.

In brief

Okubo et al. demonstrate that β-glucan binding to the glycosphingolipid lactosylceramide engages a Lyn kinase to SHP-1 phosphatase pathway that reduces FcγRIIA binding propensity for IgG, which suggests FcγRIIA affinity regulation by “inside-out” signaling. The β-glucan-lactosylceramide-Lyn axis prevents FcγRIIA-dependent neutrophil recruitment *in vitro* and to intravascular IgG deposits following glomerulonephritis.

Graphical Abstract

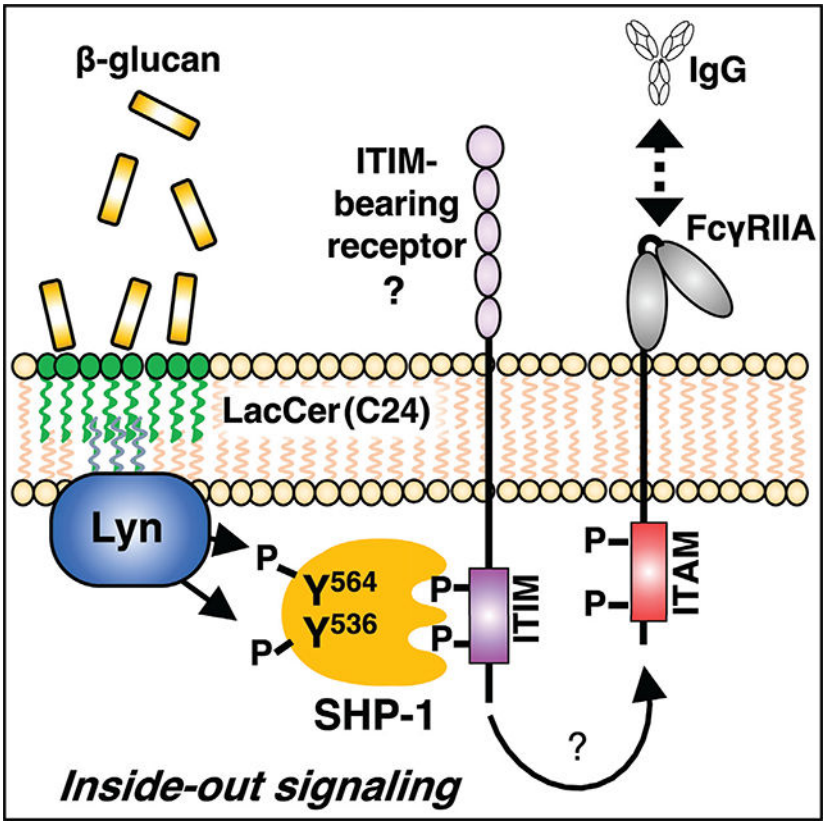

INTRODUCTION

Activating FcγRIIA and FcγRIIIB on human neutrophils have low affinity for monomeric IgG but efficiently bind antigen-complexed immunoglobulin Gs (IgGs), which promotes receptor clustering and activation of neutrophil effector functions. Single nucleotide polymorphisms (SNPs) in FcγRIIA are associated with diseases ranging from rheumatoid arthritis to sepsis (Anania et al., 2018; Beppler et al., 2016; Duits et al., 1995; Khor et al., 2011; Radstake et al., 2003; Rossi et al., 2018; Xia et al., 2018). FcγRIIA mediates destructive antibody-based inflammation (Bruhns and Jönsson, 2015) by promoting a number of neutrophil effector responses by immunoreceptor-tyrosine-based-activation motif

(ITAM)-based signaling (Ben Mkaddem et al., 2019; Wang and Jönsson, 2019). It also promotes leukocyte recruitment under physiological flow to IgG bound to the activated endothelium (Florey et al., 2007; Saggu et al., 2018)(Tsuboi et al., 2008), which mimics anti-endothelial cell antibody (AECA) deposition observed in autoimmune patients (Renaudineau et al., 2002). This recruitment requires high-affinity/valency interactions of FcγRs with IgG immune complexes (ICs) due to both low ligand density and the requirement for rapid binding under shear stress. The other low-affinity activating receptor in neutrophils is FcγRIIIB, a glycosylphosphatidyl-inositol (GPI)-linked receptor that is expressed at 8-fold higher levels than FcγRIIA (Kerntke et al., 2020) and also participates in neutrophil recruitment (Coxon et al., 2001; Florey et al., 2007), but its full physiological function remains to be elucidated (Bruhns and Jönsson, 2015).

Given the importance of FcγRIIA in several leukocyte responses, it is likely that the intrinsic binding propensity of FcγRIIA for the ligand is tightly regulated. In leukocyte CD18 integrins, engagement of heterologous receptors is well known to trigger inside-out signals culminating in conformational changes that alter the affinity of individual integrins for their ligands (Springer and Dustin, 2012). Stabilization of binding occurs by catch-bond formation, wherein forces from blood flow increases the lifetime of receptor-ligand bonds (Chen et al., 2010; Kong et al., 2009; Rosetti et al., 2015). Integrin lateral clustering at the plasma membrane also increases the number of individual interactions and therefore the overall avidity for ligands (Calderwood, 2004). In contrast to integrins, regulators of FcγR activity and function have not been well studied (Koenderman, 2019). Priming of neutrophils with granulocyte-macrophage colony-stimulating factor (GM-CSF), complement component C5a (C5a), or sphingosine-1-phosphate (S1P) clearly increases FcγRIIA-mediated binding of neutrophils to IgG-coated particles and potentiates FcγRIIA-induced reactive oxygen species (ROS) generation without altering surface levels of the receptor (Florey and Haskard, 2009; Koenderman et al., 1993; Tsuboi et al., 2011). However, the underlying mechanisms for the observed increase in FcγRIIA activity remains largely unexplored (Bracke et al., 1998).

Glycosphingolipids (GSLs) are membrane lipids containing a hydrophobic ceramide linked to at least 400 different glycan moieties, thus giving rise to a large number of structurally different compounds (Hakomori, 1981; Sud et al., 2007). GSLs form cellular membrane clustering microdomains with other sphingolipids and cholesterol, called lipid rafts (Pike, 2004), which can serve as organizing centers for signal transduction, membrane protein trafficking, cytoskeletal reorganization, and pathogen entry (Kumar et al., 2015). The GSL lactosylceramide (LacCer) (Hakomori, 1981) in human neutrophils promotes phagocytosis (Nakayama et al., 2008), ROS production and microbicidal activity, (Iwabuchi and Nagaoka, 2002; Wakshull et al., 1999) and chemotaxis (Sato et al., 2006). Moreover, LacCer directly binds to and activates Lyn kinase in detergent insoluble fractions (Iwabuchi and Nagaoka, 2002; Iwabuchi et al., 2008), but the length of the fatty acid chain matters. That is, C24 LacCer with 24 carbon atoms in its long fatty acid chain activates Lyn, whereas C16 LacCer is unable to do so (Iwabuchi et al., 2008, 2010). Lyn has activating as well as inhibitory functions (Scapini et al., 2000). A phosphorylation target of Lyn is the Src-homology-region-2-domain-containing tyrosine phosphatase 1 (SHP-1) (Mkaddem et al., 2017), which has been implicated in inhibitory signaling.

β-glucans, a major constituent of fungal, plant, and bacterial cell walls, exert immunomodulatory functions (Rahar et al., 2011). Intestinal commensal fungi under conditions of homeostasis or fungal overgrowth may release soluble β-glucan (Limon et al., 2017). As a result, anti-β-glucan antibodies, primarily IgG, are present in healthy individuals (Chan et al., 2016; Chiani et al., 2009). Particulate fungal-derived glucans are known to bind to the C-type lectin receptor Dectin-1 and elicit cellular responses (Goodridge et al., 2009). Among the several kinds of β-glucans, β−1,3/1,6 glucan derived from zymosan, a cell wall component of *Saccharomyces cerevisiae*, was reported to bind the leukocyte CD18 integrin Mac-1 (Yan et al., 1999), albeit others have shown that this is not the case (Wakshull et al., 1999). β1,6-glucan was also shown to stimulate tumoricidal activity when co-administered with anti-tumor antibody or chemotherapy (Segal et al., 2016); the underlying mechanisms for its tumoricidal activity are still being elucidated but require the presence of anti-β-glucan antibodies (Thomas et al., 2017). Interestingly, there is evidence that β−1,3/1,6 glucan, hereafter referred to as β-glucan, directly binds LacCer (Wakshull et al., 1999; Zimmerman et al., 1998), but the biological significance of this remains largely unexplored.

Here, we made the surprising discovery that in contrast to the reported activating properties of β-glucans (Poulain and Jouault, 2004), β-glucan inhibits FcγRIIA-mediated binding to complexed IgG under shear flow by interacting with the long-chain LacCer (C24:0) and sought to understand the mechanisms underlying this finding and its biological significance.

RESULTS

β-glucan inhibits human neutrophil binding to IC-coated endothelium by a LacCer-dependent mechanism

To examine the effect of β-glucan on human polymorphonuclear neutrophil (PMN) recruitment to ICs under physiological flow, we exploited two previously developed assays that identified differential requirements for FcγRIIA and FcγRIIIIB in neutrophil binding. These assays were tumor necrosis factor alpha (TNF-α)-activated human dermal microvascular endothelial cells (HDMECs) coated with a primary anti-endoglin antibody and secondary rabbit anti-endoglin that generates ICs *in situ* (referred to hereafter as IC-coated HDMECs), which increases the binding observed with TNF-α activation alone; this enhancement is FcγRIIA dependent (Florey et al., 2007; Saggu et al., 2018). On the other hand, preformed soluble ICs immobilized on coverslips capture PMNs by FcγRIIIB (Coxon et al., 2001; Florey et al., 2007). First, using a fluorophore-conjugated β-glucan, we examined β-glucan binding to PMNs and found that it bound in a dose-dependent manner with maximum binding at 100 μg/ml (Figure S1A). Next, we evaluated PMN binding to IC-coated HDMECs under physiological flow in the presence of 100 μg/ml β-glucan or the control dextran, an α1,6/1,3-glucan. β-glucan abrogated the FcγRIIA-induced enhancement of binding to TNF-α-activated, IC-coated HDMECs (Figure 1A) while having no effect on FcγRIIA surface expression levels on PMNs (Figure S1B) or PMN binding to HDMECs stimulated with TNF-α alone (Figure 1A). β-glucan-mediated inhibition was dose dependent (Figure S1C), and we confirmed that the binding to IC-coated HDMECs was FcγRIIA and not FcγRIIIB dependent (Figure S1C). β-glucan also inhibited binding to TNF-α-activated HDMECs coated with mouse anti-endoglin IgG alone (Figure S1D). Thus, β-glucan

effectively reduces FcγRIIA-mediated neutrophil recruitment to both rabbit and mouse IgG under flow.

β-glucan specifically binds to LacCer in human neutrophils with no detectable binding to other GSLs (Wakshull et al., 1999; Zimmerman et al., 1998). Thus, we examined the effect of a functional blocking antibody to LacCer, CDw17 (Zimmerman et al., 1998), on PMN binding to IC-coated HDMECs and found that it blocked the inhibitory effect of β-glucan (Figure 1A). On the other hand, we found that β-glucan had no effect on PMN binding to coverslip-immobilized ICs under flow, a FcγRIIIB-dependent process (Coxon et al., 2001; Florey et al., 2007: Figure 1B). Thus, β-glucan binds to LacCer to selectively affect FcγRIIA-mediated neutrophil binding to ICs under flow.

We found that β-glucan binding to murine neutrophils was not dependent on FcγRIIA or Mac-1 (Figure S1E), whereas binding was reduced in Dectin-1-deficient murine neutrophils (Figure S1F). Bone-marrow-derived murine neutrophils do not interact with IC-coated HDMECs (data not shown), which precluded their use in this assay. Thus, to examine the contribution of Dectin-1 to β-glucan's inhibitory effect, we assessed binding of wild-type and Dectin-1-deficient neutrophils to coverslip-immobilized ICs. This assay assesses the activity of the FcγRIIA murine ortholog FcγRIII, which also supports neutrophil binding to immobilized ICs under flow (Coxon et al., 2001). Dectin-1 deficiency had no effect on β-glucan-mediated inhibition of FcγR binding to immobilized ICs (Figure S1G). β-glucan effects were also not dependent on Toll-like receptors (TLRs), as a deficiency in MyD88/TRIF, required for TLR signaling (Roeder et al., 2004), did not affect β-glucan-induced inhibition of binding to ICs under flow (Figure S1H).

β-glucan inhibits FcγRIIA-mediated HL60 cell adhesion to ICs that is dependent on LacCer C24 with long fatty acid chains

To interrogate the role of fatty acid chain length of LacCer in β-glucan inhibitory effects on FcγRIIA activity, we used the human promyelocytic leukemic cell line HL60, which differentiates into neutrophil-like cells following dimethylformamide (DMF) treatment (Mulder et al., 1981). Unlike neutrophils, HL60 cells have a low percentage of long LacCer C24 and a high percentage of short LacCer C16 (Iwabuchi et al., 2008). This gave us the opportunity to evaluate the effects of reconstitution with LacCer of different chain lengths on cellular responses. HL60 cells do not express FcγRIIIB (Figure S2A) and have very low levels of FcγRIIA even after differentiation (Figure S2A). Given this, we engineered HL60 cells expressing levels of FcγRIIA (HL60–2A) that were only slightly lower than those in human neutrophils (Figures S2A and S2B). In cell lines, FcγRIIA can support cell binding to coverslip-immobilized ICs under flow when it is expressed in the absence of FcγRIIIB (Saggu et al., 2018). β-glucan failed to inhibit FcγRIIA-mediated adhesion of HL60–2A cells to coverslip-immobilized ICs (Figure 1C), but importantly, this was restored by pretreating HL60–2A cells with exogenous LacCer C24:0, which incorporates into the lipid bilayer (Iwabuchi et al., 2008). Similar treatments with the shorter LacCer C16 and C18 had no effect (Figure 1C). Anti-CDw17 antibody reversed the inhibitory effect of β-glucan (Figure 1C). Long LacCer C24 has one (C24:1) or no (C24:0) double bond in its fatty acid chain. HL60–2A reconstituted with C24 with either a single or double bond supported β-

glucan's inhibitory activity (Figure S3). Importantly, recruitment of LacCer-C24:0-reconstituted HL60–2A cells drawn across IC-coated HDMECs, which is also dependent on FcγRIIA for this cell line (Figure 1D), was inhibited by β-glucan (Figure 1E).

In Jurkat T cells co-expressing FcγRIIA (J-2A) and Mac-1 (J-2A Mac-1), cis interactions between Mac-1 and FcγRIIA negatively regulate cell binding to coverslip-immobilized ICs (Saggu et al., 2018). Because Mac-1 has been reported to bind β-glucan, we determined whether the inhibitory effect of β-glucan is affected by Mac-1 by using J-2A and J-2A-Mac-1 cells (Figure S4A). As with HL60 cells, LacCer C24 content is minimal in Jurkat cells (Seumois et al., 2007). Accordingly, β-glucan had no inhibitory effect on J-2A alone or J-2A-Mac-1 (Figure S4B), whereas in the absence of β-glucan, cells expressing Mac-1 significantly reduced cell binding to ICs (Figure S4B) as previously reported (Saggu et al., 2018). The addition of LacCer C24 restored the inhibitory capacity of β-glucan and further reduced binding of cells expressing Mac-1 (Figure S4B). This confirms the importance of LacCer C24 in β-glucan-mediated inhibition of FcγRIIA in an independent cell line and shows that β-glucan activity is not dependent on Mac-1.

β-glucan-mediated inhibition of FcγRIIA-dependent cell binding to ICs requires Lyn and SHP-1 and the FcγRIIA ITAM motif

Lyn kinase interdigitates with LacCer long fatty acid C24:1 and C24:0 forms (Iwabuchi et al., 2010). In neutrophils, Lyn phosphorylation of immunoreceptor tyrosine-based inhibitory motifs (ITIMs) in inhibitory receptors recruits the phosphatase SHP-1 to the membrane, thus reducing integrin signaling (Pereira and Lowell, 2003). Human neutrophils and HL60 cells express Lyn and not Fyn, which can compensate for Lyn in other immune cells (Chan et al., 1997; Saijo et al., 2003), whereas Jurkat cells (J-2A) express Fyn instead of Lyn (Figure 2A). SHP-1 is present in all three cell types (Craggs and Kellie, 2001; Garg et al., 2020). To determine whether Lyn and SHP-1 were required for β-glucan-mediated inhibition of FcγRIIA function, HL60–2A cells were transduced with Lyn or SHP-1 short hairpin RNA (shRNA) lentiviruses by using two independent sequences for each or scramble (scRNA) or non-target (ntRNA) shRNA lentivirus controls, respectively. Targeted shRNAs reduced Lyn (Figure 2B) and SHP-1 (Figure 2C) protein levels by over 90% compared to their respective control shRNAs but had no effect on FcγRIIA surface expression levels (Figure S5). Analysis of cell binding to coverslip-immobilized IC or TNF-α-activated, IC-coated HDMECs revealed that silencing of Lyn or SHP-1 had no effect on HL60–2A binding per se. On the other hand, the silencing of either molecule completely abrogated the ability of β-glucan to inhibit FcγRIIA-mediated adhesion to coverslip-immobilized ICs (Figures 2D and 2F) and IC-coated HDMECs (Figures 2E and 2G). Likewise, pharmacological inhibition of SHP-1/2 reversed the inhibitory effect of β-glucan, whereas an inhibitor of SHIP-1, an inositol lipid phosphatase, had no effect (Figure 2F). Thus, the LacCer-Lyn-SHP-1 axis is essential for the β-glucanmediated inhibition of cell binding to ICs under shear stress. To investigate the role of FcγRIIA's ITAM in β-glucan suppression of IC binding, we generated HL60 cells transduced with a ΔITAM-FcγRIIA mutant, which has a mutation in Tyr299 and 304 that promotes ITAM signaling as well as Y281, proximal to the transmembrane region, which may also support FcγRIIA signaling (Ben Mkaddem et al., 2014). HL60 cells expressing ΔITAM-FcγRIIA bound to ICs under flow but were resistant

to β-glucan treatment (Figure 2H), suggesting that the ITAM is not required for FcγRIIA-mediated binding per se but is required for β-glucan's inhibitory effect.

β-glucan treatment induces Lyn-dependent SHP-1 phosphorylation and complex formation

SHP-1 binds the ITAM of human FcγRIIA to prevent Syk-mediated phosphorylation of ITAM-Y304 and subsequent ROS production and cytokine release (Ben Mkaddem et al., 2014). SHP-1 Y536 and Y564 phosphorylation activate the phosphatase and are potential phosphorylation sites for Lyn (Ben Mkaddem et al., 2019). We found that β-glucan treatment induced the phosphorylation of both Y536 and Y564 in HL60–2A cells reconstituted with LacCer C24 (Figure 3A). Similar results were obtained with human neutrophils (Figure 3B). β-glucan-induced SHP-1 phosphorylation required LacCer C24 and was reduced in Lyn knocked down cells (Figure 3C). Immunoprecipitation of SHP-1 showed that β-glucan enhanced Lyn binding to SHP-1 in the presence of LacCer C24 but not LacCer C16 (Figure 3D). Moreover, the Lyn-associated SHP-1 was phosphorylated on Y536 and Y564, suggesting activation of the phosphatase (Figure 3D). Lyn is usually found in the Triton-X extractable, cytosolic fraction of neutrophils (Kovárová et al., 2001; Borzęcka-Solarz et al., 2017; Figure 3E). β-glucan treatment in the presence of LacCer C24 decreased Triton X-100 extractability of Lyn, which suggests translocation of a portion of intracellular Lyn to more detergent-resistant membrane fractions following β-glucan treatment (Figure 3E). As Lyn has been shown to be recovered specifically in LacCer-rich membranes of HL60 cells loaded with C24 but not C16 (Iwabuchi et al., 2008), our results imply that β-glucan treatment leads to greater association of Lyn with C24 containing membrane microdomains. The observed Lyn translocation did not occur in LacCer-C16-loaded cells. The conclusions from data shown in Figure 3E are as follows. First, in β-glucan-treated HL60–2A cells, Lyn is less detergent soluble when cells are loaded with C24, whereas it is readily extractable in C16-loaded cells, which is consistent with our model of increased recruitment of Lyn to LacCer-C24-containing microdomains in the presence of β-glucan. Second, a comparison of HL60–2A cells loaded with C24 shows that β-glucan reduces Lyn extractability compared to dextran treatment, indicating that β-glucan but not the control dextran induces the partitioning of Lyn to more detergent-resistant fractions. In summary, in the presence of LacCer C24, β-glucan promotes Lyn translocation to detergent-resistant membrane compartments as well as the association with SHP-1, leading to phosphorylation and activation of this tyrosine phosphatase.

FcγRIIA effective 2D affinity for IgG is reduced by β-glucan

To determine whether β-glucan affects FcγRIIA affinity for IgG, we assessed the effective 2D affinity of hIgG binding to FcγRIIA on the cell surface with a micropipette adhesion frequency assay (Chesla et al., 1998). This assay has the sensitivity of detecting a single FcγRIIA-IgG bond but does not require the discrete adhesion events to be single-bond events. Binding to IgG ICs was specific for cells treated with vehicle or β-glucan in cells loaded with C16 LacCer or C24 LacCer because not coating red blood cells (RBCs) with hIgG abolished adhesion (Figure 4A). Binding affinity was significantly reduced by β-glucan when C24 LacCer, but not C16 LacCer, was present (Figure 4A). We next measured the effect of Lyn on FcγRIIA-IgG affinity in C24-loaded cells. In the absence of β-glucan, there was no significant difference between scRNA control and Lyn shRNA HL60–2A cells

(Figure 4B), suggesting that Lyn does not tonically affect FcγRIIA-IgG affinity. After the addition of β-glucan to the scRNA control sample, there was a decrease in specific hIgG affinity (Figure 4B). In contrast, shRNA knockdown of Lyn did not result in a similar reduction. In fact, it significantly increased the effective 2D affinity of FcγRIIA for hIgG in the presence of β-glucan compared to Lyn-silenced cells without β-glucan (Figure 4B). To obtain the A_cK_a values, which is the effective 2D affinity as defined in the STAR Methods, the measured adhesion frequencies were corrected for any variations in FcγRIIA and hIgG site densities. Thus, β-glucan lowers FcγRIIA affinity for IgG only in the presence of Lyn. We posit that the observed increase in apparent FcγRIIA-IgG 2D affinity in the absence of Lyn may be the result of unopposed β-glucan-induced signaling by LacCer that results in an increase in FcγRIIA affinity for IgG.

To determine whether SHP-1 also regulates FcγRIIA-IgG 2D affinity, we performed micropipette experiments using ntRNA control and SHP-1 shRNA HL60–2A cells in the presence or absence of β-glucan (Figure 4C). Although β-glucan reduced FcγRIIA affinity for IgG in ntRNA control cells, it did not in SHP-1 shRNA cells. Thus, like Lyn, SHP-1 is required for β-glucan-induced modulation of FcγRIIA 2D affinity for ligand. However, unexpectedly, a reduction in FcγRIIA affinity for IgG in SHP-1 shRNA compared to ntRNA control was also observed in the absence of β-glucan, which suggests a role for SHP-1 in FcγRIIA affinity regulation under steady-state conditions. This was not reflected in our flow assays wherein SHP-1 silencing had no effect on FcγRIIA-IgG interactions (Figures 2F and 2G). The likely reason for this discrepancy is that the micropipette adhesion frequency assay measures FcγRIIA-IgG Fc binding affinity in the absence of externally applied forces. In comparison, the read out of the flow chamber depends on both the affinity and dissociation off-rate under the force exerted by shear flow, with a more minor dependence on affinity (Yago et al., 2008; Zhu et al., 2008). As such, the two assays may not give identical results.

The contact between the two cells had an apparent area of A_c ~3 μm^2, which contained ~750 FcγRIIA and ~480 IgG molecules, on average, given their respective site densities of ~260 FcγRIIA and ~160 IgG molecules per μm^2 as determined by flow cytometry. We interpreted the cell adhesion frequency data by using a model of bimolecular interaction kinetics (between one FcγRIIA and one IgG to form one bond) to evaluate an effective 2D affinity A_cK_a from fitting the model to the data in a fashion as fitting a similar model to the sensorgrams generated using surface plasmon resonant (SPR) technology. In the SPR experiment, if the IgG is aggregated, the value returned from using a monomeric interaction model to curve-fit the binding sensorgrams would reflect multimeric binding avidity rather than a true monomeric binding affinity (Li et al., 2007). The same issue also exists here. We have previously performed Monte Carlo simulations to demonstrate the cooperativity condition required for the adhesion frequency assay to report avidity rather than affinity (Huang et al., 2010). In essence, although the adhesion measured by our assay may be mediated by multiple bonds or even a cluster of bonds due the possible clustering of FcγRIIA on the HL60–2A cell membrane, the monomeric binding model is still applicable and the fitted parameter still represents affinity rather than avidity, provided that no cooperativity or synergy exists among monomeric members in the clusters. By cooperativity, we mean that engagement of one monomeric member would enhance the propensity of other members in the same cluster to bind ligands (Huang et al., 2010).

β-glucan has no effect on FcγR-cross-linking-induced generation of ROS and cell spreading

To examine β-glucan's role in modulating events after FcγR engagement and clustering, we examined cell spreading on immobilized ICs, which is FcγRIIA (Xiong et al., 2006), Mac-1 (Tang et al., 1997), and lipid raft (Bournazos et al., 2009) dependent, and ROS generation after directly cross-linking FcγRIIA with anti-FcγRIIA antibody, which leads to FcγR clustering and subsequent ITAM-based signal transduction (Wang and Jönsson, 2019). Both assays bypass any contribution of FcγR affinity changes to observed outcomes. β-glucan had no effect on FcγRIIA-dependent cell spreading on immobilized ICs (Figure 5A). Likewise, Lyn deficiency did not increase FcγRIIA-dependent cell spreading after β-glucan treatment and, in fact, exhibited less spreading independent of β-glucan stimulation (Figure 5B). Clustering of FcγRs in neutrophils by cross-linking them with an antibody activates NADPH oxidase and results in the generation of ROS (Crockett-Torabi and Fantone, 1990). β-glucan failed to inhibit FcγRIIA-cross-linking-induced generation of ROS both in human neutrophils (Figure 5C) and in LacCer-C24:0-treated HL60–2A cells (Figure 5D). Thus, β-glucan does not inhibit responses following high valency engagement of FcγRIIA. Lyn, irrespective of its role in β-glucan-mediated signaling per se, was required for FcγRIIA-cross-linking-induced ROS generation (Figure 5E). Thus, Lyn has opposing regulatory roles, as follows: it is required for inside-out, β-glucan-LacCer-C24-induced inhibition of FcγRIIA affinity for IgG but then promotes cell spreading and ROS generation after FcγRIIA engagement and clustering independent of β-glucan treatment. This is consistent with the known dual roles for Lyn kinase in other myeloid cell types (Scapini et al., 2009). We also observed no effect of β-glucan on FcγRIIA-mediated phagocytosis of IgG-coated targets (Figure 5F), a process that requires ITAM signaling (Kim et al., 2001) and, accordingly, was absent in the ΔITAM-FcγRIIA cells (Figure 5F).

β-glucan inhibits renal neutrophil infiltration after acute antibody-mediated glomerulonephritis by a GSL- and Lyn-dependent process

Acute, nephrotoxic serum (NTS) nephritis results in the generation of IgG-ICs within glomerular capillaries and subsequent rapid neutrophil recruitment that is ameliorated in mice lacking all their endogenous activating FcγRs (γ-chain deficient) or FcγRIII (Coxon et al., 2001), a closely related ortholog to human FcγRIIA (Nimmerjahn and Ravetch, 2006). The glomerular neutrophil recruitment is restored when human FcγRIIA is expressed selectively on neutrophils of γ-chain-deficient mice (Tsuboi et al., 2008). β-glucan treatment of wild-type mice significantly ameliorated the early rise in neutrophil influx (Figure 6A). To examine the role of LacCer on neutrophil recruitment, mice were treated with myriocin, a specific pharmacological inhibitor of serine palmitoyltransferase that synthesizes ceramides (precursors of LacCer) and decreases ceramide levels (Kurek et al., 2014), including C24 ceramides (Walls et al., 2018), when administered *in vivo*. Myriocin treatment completely reversed the inhibitory effect of β-glucan on neutrophil recruitment (Figure 6B). Glomerular neutrophil accumulation in NTS nephritis was largely unaffected in Lyn-deficient mice, but β-glucan-mediated inhibition of neutrophil recruitment was completely reversed in these mice (Figure 6C). Mice expressing human FcγRIIA (RIIAtg/$\gamma^{-/-}$ mice) (Tsuboi et al., 2008) were treated with β-glucan and subjected to NTS nephritis. β-glucan significantly inhibited FcγRIIA-induced neutrophil recruitment (Figure 6D) that was reversed by

myriocin treatment (Figure 6E). Together, these data provide *in vivo* evidence that binding of β-glucan to LacCer on neutrophils inhibits FcγR-dependent neutrophil recruitment in the kidney in a Lyn-dependent manner.

The reverse passive Arthus (RPA) reaction is elicited by the generation of ICs primarily in extravascular tissue and the subsequent FcγR-mediated neutrophil cytotoxic responses that induce skin edema (Sylvestre and Ravetch, 1994; Tsuboi et al., 2008). β-glucan treatment of wild-type mice had no effect on edema evaluated by leakage of Evans blue dye or on neutrophil accumulation (Figure 6F). Similarly, β-glucan treatment of mice expressing human FcγRIIA (RIIAtg/$\gamma^{-/-}$ mice) had no effect on Evans blue leakage (Figure 6G).

DISCUSSION

Our study demonstrates that the binding propensity of FcγRIIA for IgG-ICs is negatively regulated by signals resulting from the binding of a fungal-derived soluble β1,6-glucan to the GSL LacCer. This binding propensity was assessed by evaluating neutrophil binding to IC-coated endothelial cells under shear flow conditions and, more directly, by using the micropipette adhesion frequency assay (Chesla et al., 1998), which measures the likelihood of adhesion between a FcγRIIA-expressing cell and an human-IgG-coated RBC. β-glucan/LacCer signaling may induce putative conformational changes in FcγRIIA (Sondermann et al., 2001) to decrease affinity and/or reduce the FcγRIIA clusters' capacity for cooperative binding to decrease avidity. Notably, distinguishing these possibilities will be a challenge because even in the case of integrins, definitive proof of cooperativity among individual integrin molecules in a cluster is difficult to obtain (Carman and Springer, 2003; Stewart and Hogg, 1996). With this caveat in mind, here, "affinity" refers to the "effective 2D affinity," which is a gauge of the FcγRIIA-IgG Fc binding propensity measured in the cellular context.

We demonstrate that a defined intracellular signaling pathway triggered by engagement of LacCer regulates FcγR affinity for IgG, a process functionally referred to as inside-out signaling (as depicted in Figure S6) that is well described for b2 integrins. Distinct from the analogies to integrin activation by inside-out signals, we define a negative regulatory axis triggered by β-glucan-LacCer C24 that reduces FcγRIIA affinity for IgG-ICs and subsequent IC-mediated neutrophil recruitment *in vitro* and *in vivo*. This represents a new mechanism for regulating FcγR-IgG interactions aside from the described role of IgG subclass and N-glycosylation in regulating FcγR affinity/avidity for IgG (Patel et al., 2019). Current studies were conducted with rabbit and mouse IgG for adhesion assays under flow and human IgG1 for affinity measurements; future studies are needed to understand whether the β-glucan/LacCer axis described here similarly modulates FcγRIIA binding to human IgGs of different subtypes and glycosylation profiles (Patel et al., 2019). β-glucan had no effect on events after direct FcγR engagement or integrin-mediated functions such as neutrophil recruitment to TNF-α-activated endothelium *in vitro* under flow or *in vivo*, in the RPA (Florey et al., 2007; Norman et al., 2003). This suggests that β-glucan/LacCer selectively regulates signaling events that modulate FcγR binding to the ligand. We predict that the mechanisms described in our studies will only be relevant under conditions in which high-affinity interactions between FcγR and ligand are needed to induce effector responses.

Accordingly, the described tethering of neutrophils and monocytes under physiological flow conditions to a discrete amount of deposited IgG-ICs would be regulated by the mechanisms described here. It may also be relevant when neutrophils or monocytes need to capture sub-optimally opsonized, mobile pathogens.

How is the FcγRIIA activity regulated by β-glucan-LacCer? We show that β-glucan binding to long-chained LacCer 24:0 triggers Lyn-mediated phosphorylation of SHP-1 at both Y536 and Y564, which are known to relieve basal inhibition of SHP-1 (Abram and Lowell, 2017). This in turn could lead to the dephosphorylation of the ITAM of FcγRIIA, which is a known target site of SHP-1 (Ben Mkaddem et al., 2014) and shown to be required for β-glucan-induced inhibition of FcγRIIA-dependent binding to ICs under shear flow. Notably, full activation of SHP-1 phosphatase activity also requires the binding of its SH2 domains to pTyr-containing substrates, in particular proteins that contain ITIM sequences, which are found in the cytoplasmic domain of many cell surface inhibitory receptors in myeloid cells (Favier, 2016). Thus, an intervening ITIM-containing protein (receptor or intracellular protein) may be required for full SHP-1 activity after LacCer engagement. SHP-1 dephosphorylates tyrosine residues in ITAMs. Accordingly, FcγRIIA lacking this motif failed to respond to β-glucan/LacCer-mediated inhibition under flow. However, it did not impact FcγRIIA-mediated binding to ICs in the absence of β-glucan, which suggests that ITAM phosphorylation per se does not contribute to the basal FcγRIIA affinity for IgG, which likely relies solely on the extracellular domain. Thus, the β-glucan/LacCer-triggered inside-out signaling impinges on the ITAM to decrease the ability of the extracellular domain to bind the ligand. The β-glucan/Lyn and the published paradoxical monomeric IgG-ITAM inhibitory signaling converge at the level of SHP-1. β-glucan engagement of a GSL, LacCer, stably recruits SHP-1 to inhibit FcγRIIA affinity for the ligand, whereas monomeric IgG engagement of the FcγRIIA receptor itself also triggers stable SHP-1 activation to prevent downstream ITAM-based signaling (Ben Mkaddem et al., 2014; Pfirsch-Maisonnas et al., 2011). It is possible that a common pathway downstream of SHP-1 is triggered by these two distinct upstream inputs and associated signaling events. Unlike human neutrophils, the FcγRIIA-expressing HL60 cells used in our studies to interrogate the aforementioned signaling pathways do not express FcγRIIIB. However, given that FcγRIIIB is a GPI-linked receptor that lacks ITAM signaling, the FcγRIIA regulatory mechanisms proposed in our studies are not expected to be affected by FcγRIIIB.

Consistent with the effect of β-glucan on FcγRIIA affinity, β-glucan reduced neutrophil recruitment after NTS nephritis *in vivo* or IC deposition on TNF-α-activated HDMECs *in vitro* under flow, both of which depend on FcγR-mediated adhesion events (Florey et al., 2007; Saggu et al., 2018). Evidence that the inhibitory effect of β-glucan on neutrophil recruitment requires LacCer is the reversal of the effect *in vitro* by an antibody to LacCer. *In vivo* treatment of mice with myriocin, which inhibits ceramides synthesis, also prevented β-glucan-mediated inhibition, albeit in this case, we cannot conclude that the observed effects were specifically due to the absence of LacCer. On the other hand, β-glucan did not affect neutrophil recruitment in the RPA model or to TNF-α-activated HDMECs, which rely on selectin-mediated neutrophil rolling and integrin-dependent firm adhesion (Florey et al., 2007; Norman et al., 2003). It is possible that the reduction in FcγR-mediated binding to IgG and subsequent activation of Mac-1 integrin (Ortiz-Stern and Rosales, 2003) contribute

to the overall reduction in cell adhesion, as Mac-1 is required for sustained neutrophil accumulation in NTS nephritis (Tang et al., 1997) and, in vitro, firm adhesion to IC-coated HDMECs (Florey et al., 2007). Importantly, β-glucan treatment had no effect on neutrophil-mediated tissue damage in the RPA reaction, which is dependent on FcγR-dependent cytotoxic responses primarily in extravascular tissues (Sylvestre and Ravetch, 1994, 1996; Tsuboi et al., 2008; Utomo et al., 2008). This is likely, as these responses are triggered by FcγR engagement with the high density, complexed ligand under relatively static conditions and therefore are unaffected by changes in FcγRIIA affinity. Furthermore, β-glucan does not influence steps after FcγR binding to the ligand (as depicted in Figure S6).

Yeast-derived soluble β-glucan has been shown to improve survival in cancer patients by complexing with naturally occurring IgG anti-β-glucan antibodies (Thomas et al., 2017). β-glucan binds to Dectin-1 (Goodridge et al., 2009) and may (Yan et al., 1999) or may not (Wakshull et al., 1999) interact with Mac-1. We found that β-glucan-induced inhibition of FcγRIIA binding to ICs is not dependent on these two receptors. Instead, β-glucan binding to LacCer C24 is specifically required for β-glucan's inhibitory activity on FcγRIIA. This is noteworthy, as LacCer, which is enriched in neutrophils and forms LacCer-rich lipid rafts (Hakomori, 2002), specifically binds β-glucan (Wakshull et al., 1999; Zimmerman et al., 1998) and has been previously reported to promote neutrophil functions (Iwabuchi and Nagaoka, 2002; Nakayama et al., 2008; Wakshull et al., 1999). The negative regulatory role for LacCer described in our studies could represent a mechanism by which soluble pathogen components, such as β-glucan released from fungi during maturation (Ishibashi et al., 2010), impair IC-induced neutrophil recruitment and subsequent fungal clearance. We show that β-glucan has inhibitory effects only upon binding to LacCer with long fatty acid chains, which are needed for Lyn recruitment (Iwabuchi et al., 2008). It is possible that a change in the abundance of long- versus short-chained C24 could, in *trans*, increase pro-inflammatory outcomes after β-glucan stimulation. Enhanced LacCer C24 serum levels were observed in children with ulcerative colitis and suggested as a biomarker (Filimoniuk et al., 2020). In a mouse model of the autoimmune disease lupus nephritis, altered GSL metabolism led to renal accumulation of LacCer, particularly C24 (Nowling et al., 2015); and elevated β−1,4 GalT-V, an enzyme that synthesizes LacCer, was elevated in lupus patients (Sadras et al., 2020). In a model of skin inflammation in atherosclerosis, elevated LacCer was proposed to contribute to neutrophil infiltration, leading to tissue damage (Bedja et al., 2018).

Lyn and SHP-1 play important roles in maintaining immune homeostasis. Older Lyn-deficient mice develop mild lupus-like kidney disease (Hibbs et al., 1995), whereas conditional deletion of SHP-1 in neutrophils results in excessive inflammation linked to enhanced integrin signaling (Abram et al., 2013). Lyn deficiency alone, in the absence of β-glucan, had no effect on FcγRIIA-IgG interactions *in vitro* and did not exhibit significantly increased neutrophil accumulation after acute, NTS nephritis *in vivo*. Thus, Lyn is not a tonic inhibitor of FcγRIIA effective 2D affinity for IgG. The higher effective 2D affinity of FcγRIIA for IgG after β-glucan treatment in the absence of Lyn indicates that Lyn may serve as a gateway to uncontrolled activation during fungal infection. Likewise, SHP-1 silencing averted β-glucan-induced reduction in FcγRIIA affinity for IgG. Surprisingly, SHP-1 silencing reduced the 2D affinity of IgG in the absence of β-glucan. It is possible that the tonic loss of SHP-1 results in compensatory upregulation of other inhibitory receptors,

such as FcγRIIB, which could directly inhibit FcγRIIA function and thus help maintain tonic signaling levels in resting cells but be less relevant in β-glucan-stimulated cells. Compensatory modulation of signaling pathways in gene knockout lymphocytes has been reported (Bittner et al., 2015; Folgosa et al., 2013). On the other hand, SHP-1 may positively regulate FcγRIIA, as has been shown in macrophages wherein SHP-1 promotes TLR-induced interleukin-12p40 (IL-12p40) production by phosphatidylinositol 3-kinase (PI3K) activation (Zhou et al., 2010). Receptor clustering induced by high avidity ligand interaction induces ITAM phosphorylation that links to neutrophil cytotoxic responses such as ROS generation and phagocytosis. β-glucan treatment had no effect on these functions.

In summary, our work has identified a pathway for modulating FcγRIIA affinity for IgG that is distinct from previously described mechanisms of FcγRIIA affinity/avidity modulation (e.g., IgG subclass or FcγRIIA glycosylation) (Hayes et al., 2014). Our work demonstrates that β-glucan/LacCer regulates FcγR effective 2D affinity through an inside-out signaling pathway and thus shows an unexpected additional layer of regulation of FcγRIIA affinity for IgG. Moreover, the canonical role of β-glucan as a pathogen associated molecular pattern (PAMP) molecule is to activate innate immunity, a property that has led to the development of β-glucan as a therapeutic for cancer (Segal et al., 2016; Thomas et al., 2017). Our studies reveal a unanticipated inhibitory role for β-glucan by a LacCer-Lyn-SHP-1 axis in dampening the immune response by curtailing IC-mediated neutrophil recruitment, one of the most proximal events in inflammation. Our studies suggest that β-glucan may be contemplated as a therapeutic for IgG-mediated autoimmune diseases. However, further work is needed in this area, as it is possible that the naturally occurring anti-β-glucan antibodies (Thomas et al., 2017) could generate β-glucan-IgG-ICs that interfere with β-glucan binding to LacCer *in vivo*.

STAR★METHODS

RESOURCE AVAILABILITY

Lead contact—Further information and requests for resources and reagents should be directed to and will be fulfilled by the Lead Contact, Tanya N. Mayadas (tmayadas@rics.bwh.harvard.edu).

Materials availability—β-glucan and dextran were provided by Immuno Research and gifted for this study. Mouse lines (RIIAtg/$\gamma^{-/-}$, Mac-1 knock-out) were generated and maintained in HIM animal housing facility at Brigham and Women's Hospital, and not commercially available. Lyn knock-out mice were generated in University of California by Dr. Lowell and gifted for this study. Plasmids used for this study have been deposited to Addgene, #12254, #12260 and #12259. Cell lines generated by using these plasmids are maintained in department of pathology at Brigham and Women's Hospital.

Data and code availability—This study did not generate any unpublished custom code, software, or algorithm.

EXPERIMENTAL MODEL AND SUBJECT DETAILS

Mice—Wild-type mice (C57/BL6j), mice expressing human FcγRIIA on the neutrophils of $\gamma^{-/-}$ mice (RIIAtg/$\gamma^{-/-}$) (Tsuboi et al., 2008), Mac-1 (Coxon et al., 1996), Dectin-1 (Clec7a/J, The Jackson Laboratory), MyD88/TRIF (Yamamoto et al., 2003), and Lyn (Pereira and Lowell, 2003) knock-out mice were maintained in a specific pathogen-free facility at the HIM animal housing facility at Brigham and Women's Hospital. Mice used for experiments were 10–19 weeks old and age and sex matched. The Brigham and Women's Hospital Animal Care and Use Committee approved all procedures in this study.

Human samples—Blood samples were obtained from consented healthy volunteers and according to a Mass General Brigham Institutional Review Board (IRB)-approved protocol (1999P001694). Donors were adults of all genders, but age and sex were not noted.

METHOD DETAILS

Reagents and antibodies—TNFα (Peprotech, 10 ng/mL), SHIP-1 inhibitor (Echelon, 30 μM), SHP-1/2 inhibitor (Tocris, 500 nM), C24:1, C24:0, C18:0, C16:0 LacCer (Avanti, 2.5 μg/mL) were purchased. β-glucan (1,3–1,6 β-glucan, 10–300 μg/mL), DTAF fluorophore-conjugated β-glucan (10–300 μg/mL) and dextran (100 μg/mL) were obtained from Immuno Research. Anti-human CD32 clone IV.3 (StemCell Technologies, Inc., 60012), IgG2b isotype control (Invitrogen, MG2B00), anti-human CD16 clone 3G8 (Biolegend, 302002), IgG1 isotype control (BD, 557273), and anti-CDw17 (MyBiosource, MBS439045) antibody were used at 10 μg/mL. For adhesion assays, soluble ICs were made from BSA and anti-BSA antibody (Sigma-Aldrich, B7276). Anti-endoglin/CD105 (Biolegend, 323202) and rabbit anti-mouse (Dako, Z0259) antibodies were used at 1:250 (2 μg/mL) and 1:500 (4 μg/mL) respectively or anti-endoglin was used alone at 1:125 (4 μg/mL). For confocal microscopy, anti-Ly6G (Biolegend, 127602) was used at 1:100 and DAPI (Invitrogen) was used at 1:500. For cytometric analysis, FITC-anti-CD16 (BD, 555406), FITC-anti-CD32 (BD, 555448), PE/Cy7-anti-CD11b (Biolegend, 101216), FITC-anti-CD11b (Biolegend, 101206), PE/Cy7-anti-CD45 (Biolegend, 103114), APC-anti-Ly6G (Biolegend, 127614), and PerCP/Cy5.5-anti-Ly6C (Biolegend, 128012) antibody were used at 1:100 dilution. For western blotting, anti-Lyn (Cell signaling, 2796T), anti-Fyn (Cell signaling, 4023T), anti-pSHP-1 Y536 (ECM Bioscience, SP1571), and anti-pSHP-1 Y564 (Cell signaling, 8849) were used at 1:1000. Anti-SHP-1 (LifeSpan BioSciences, LS-C358839) antibody was used at 1:500, and anti-actin (Sigma-Aldrich, A5316) at 1:2000. Mouse anti-SHP-1 (Santa Cruz, sc7289) was used at 3 μg/mL for immunoprecipitation.

Mouse and human neutrophil isolation—Human polymorphonuclear neutrophils were isolated from whole blood using a histopaque separation method followed by dextran sedimentation of RBCs as described (Coxon et al., 2001). Mouse bone marrow neutrophils (BMNs) were isolated from mouse femurs and tibias by percoll gradient separation.

Generation of FcγRIIA mutant and transduction of shRNA with lentivirus in HL60 and Jurkat cells—Human FcγRIIA or FcγRIIA with mutations in the ITAM motif (Tyr299 and 304) and the cytoplasmic tail (Tyr281)(ΔITAM-FcγRIIA) were generated by site directed mutagenesis and cloned into the lentiviral plasmid pWPI (modified from the

Addgene, plasmid #12254 by removing the EGFP cassette). HEK293T cells (ATCC) were transfected with the lentiviral construct (pWPI) and plasmids psPAX2 and pMD2.G (Addgene, #12260 and #12259) using Lipofectamine (Invitrogen). Supernatant of transfected cells were used to transduce HL60 cells (ATCC) or Jurkat cells as described (Saggu et al., 2018). Cell lines were sorted on a BD FACS Aria to obtain populations with similar levels of FcγRIIA.

Sequence-verified small hairpin RNA (shRNA) lentiviral plasmids targeting Lyn (Sigma-Aldrich, TRCN0000230901, and TRCN0000218210) or SHP-1 (Sigma-Aldrich, TRCN0000235432, and TRCN0000244305) were used. Lentiviral plasmids SHC001 and SHC002 (Sigma-Aldrich) were used for generating Lyn- and SHP-1-shRNA control lines, respectively. HEK293T cells were transfected with lentiviral construct as described above. Viral transduced HL60–2A cells were then cultured for 48 hours and selected with 6.0 μg/mL puromycin for 5 days in RPMI 1640 with 10% FBS, L-glutamine, and penicillin/streptomycin. Cells were differentiated using 0.8% dimethylformamide (DMF; Sigma-Aldrich) for 4 days.

Adhesion assay under shear stress—Glass coverslips were incubated with preformed soluble BSA-anti-BSA immune complexes (sIC), mounted on a parallel plate flow chamber and perfused with cells at 37°C as described (Coxon et al., 2001; Stokol et al., 2004). Cells were perfused at 1×10^6/mL for hPMNs, BMNs and Jurkat cells or 2×10^6/mL for HL60 cells, at 1.0 dynes/cm^2 for hPMNs and Jurkat cells, 0.5 dynes/cm^2 for BMNs and HL60 cells in RPMI 0.1% BSA medium.

For binding to IC formed on human dermal microvascular endothelial cells (HDMECs, Lonza), confluent monolayers grown on coverslips were activated with human TNFα for 4 hours, incubated with anti-endoglin/CD105 antibody and subsequently with rabbit anti-mouse IgG for 15 minutes at 37°C. Cells (1×10^6/mL hPMNs or 2×10^6/mL HL60) were perfused at 1.0 dynes/cm^2 in RPMI, 1% FCS.

After 1 min of flow, adherent cells in four random fields were visualized for 10 s per coverslip, counted, and averaged. Live imaging of cell adhesion was recorded on a Nikon a TE2000 inverted microscope (equipped with a 20 × /0.75 NA phase contrast objective) coupled to a video camera.

Analysis of cell spreading under static conditions—1.5×10^5 HL60 cells in RPMI 0.1% BSA were seeded onto IC-coated coverslips for 30 minutes at 37°C, which were then gently washed with PBS, fixed with 1% Glutaraldehyde, permeabilized, and stained with Alexa 568 phalloidin to stain the actin cytoskeleton. Cell area was calculated by ImageJ (NIH) and the values of 20 cells were averaged.

FcγR cross-linking-induced generation of ROS—3×10^6 human neutrophils or 4×10^6 HL60 cells suspended in PBS without Ca^{2+}/Mg^{2+}, were incubated with mouse anti-human FcγRIIA (10 μg/mL, StemCell Technologies) on ice for 30 minutes. After pretreatment with indicated reagents at 37°C for 30 minutes, luminol (0.82 mM) in PBS with Ca^{2+}/Mg^{2+} was added, followed by the addition of secondary antibody, goat anti-

mouse F(ab') (20 μg/mL, Jackson ImmunoResearch, 115–006-006). ROS generation (expressed in relative light units, RLU) was continuously monitored using Monolight 2010 (Analytical Luminescense Laboratory). The peak level of ROS for each condition was normalized to the average of secondary antibody-untreated sample.

Flow cytometry—Flow cytometry was performed on a FACS Canto II analyzer (BD Bioscience) and data was analyzed using FlowJo (Version10.4.2). Cells were suspended in PBS plus 2% FCS and 2mM EDTA, incubated with fluorochrome-conjugated antibodies, washed with PBS and fixed in 1% paraformaldehyde.

Western blot analysis and Immunoprecipitation—Cells were treated with 2.5 μg/mL LacCer C24:0, 100 μg/mL β-glucan, or dextran for 30 mins, washed with ice cold PBS, boiled in sample buffer with protease inhibitors and subjected to SDS-PAGE and western blot analysis (Nishi et al., 2017). To obtain extractable detergent resistant fractions, cells were lysed with ice-cold cell lysis buffer (150 mM NaCl, 50 mM Tris, 1mM EDTA, protease inhibitor cocktail, and phosphatase inhibitor cocktail) containing 1.0, 0.5, 0.1, or 0.05% of Triton X-100, centrifuged and supernatants were subjected to SDS-PAGE and western blot analysis.

For immunoprecipitation studies, cells were treated with 2.5 μg/mL LacCer C24 or C16, and 100 μg/mL β-glucan or dextran for 30 mins, washed with ice-cold PBS, and lysed with ice-cold cell lysis buffer (150 mM NaCl, 50 mM Tris, 1mM EDTA, 5% Glycerol, 1% Triton X-100, protease inhibitor cocktail, and phosphatase inhibitor cocktail) and centrifuged. Supernatants were incubated with 3 μg/mL mouse anti-SHP-1 Ab for 4 hours, and 25 μL of Protein G Dynabeads (Thermo Fisher) for 30 minutes, and after washing, immunoprecipitated proteins were prepared for SDS-PAGE and western blot analysis.

Phagocytosis assay—2×10^6 HL60–2A cells were treated with LacCer C24, anti-CD32 antibody (IV.3) or isotype control, and β-glucan or dextran for 30 mins. Cells were incubated with IgG-FITC coated latex beads (Cayman Chemical) for 30 mins, washed, and quenched with trypan blue solution. The number of FITC-positive cells were counted using FACs and normalized to total cells.

Micropipette affinity experiments of FcγR-IgG adhesion—Human red blood cells (RBCs) isolated from healthy volunteers, according to protocols approved by the Institutional Review Board of the Georgia Institute of Technology, were biotinylated as described. RBCs were then incubated with 1 mg/mL streptavidin (SA) for 30 min at 15°C while shaking. SA-coated RBCs were then incubated with 20 μg/mL biotinylated human IgG1 (Novus Biologicals, NBP1–96855) for 1 hr at 15°C while shaking. RBCs were incubated in FACS buffer and 10 μg/mL Goat $F(ab')_2$ anti-human IgG Fc PE (Abcam, ab98596) for flow cytometry measurements with an Accuri C6 plus autosampler (BD). FcγRIIA levels on HL60–2A cells were determined by FACs analysis using PE anti-human CD32 (BD, 550586) or IgG2bk isotype control (BD, 555743). Site density was determined using QuantiBRITE PE Fluorescence Quantitation kits (BD, 340495). 1×10^6 HL60–2A cells, including knock-down sub-clone and scrambled RNA control cells for SHP-1 and Lyn-1, were differentiated in 0.8% DMF for 4 days were resuspended in PBS containing β-

glucan (100 μg/mL) or dextran (100 μg/mL) and C16 or C24 LacCer (2.5 μg/mL) or vehicle (PBS and 3:1; chloroform: methanol) for 30 min at 37°. After incubation, cells were added to micropipette chambers as described (Chesla et al., 1998; Zarnitsyna and Zhu, 2011). Briefly, cell pairs held under pressure by borosilicate micropipettes cut to tip diameters between 1.5 (RBCs) and 3 μm (HL60–2A cells) were brought into contact via a piezo translator for a constant duration of 2 s. Cells were then pulled apart and adhesion events were recorded via video monitor for 50 consecutive interactions between each cell pair. The adhesion frequency (P_a) was normalized to account for site densities of hIgG and FcγRIIA with a log transformation as described previously (Huang et al., 2010).

$$P_a = 1 - \exp\{-m_r m_l A_c K_a[1 - \exp(-k_{\text{off}}\, t_c)]\}$$
$$-\ln(1 - P_a)/(m_r m_l) = A_c K_a[1 - \exp(-k_{\text{off}}\, t_c)]$$
$$-\ln[1 - P_a(\infty)] = A_c K_a \cdot m_r m_l \text{ with } (t_c \to \infty)$$

with $P_a(\infty)$ the adhesion frequency at equilibrium. Here, m_r and m_l are site densities of FcγRIIA and hIgG, respectively, in #/μm^2 (determined from flow cytometry). A_c and t_c are contact area and time, and K_a and k_{off} are 2D binding affinity and off rate.

Reverse passive arthus (RPA) reaction—Mice were pretreated with 40 μg/mouse i.v. of β-glucan, or dextran. 1 hour later, rabbit anti-chicken egg albumin IgG (60 μg/30 μL, Sigma-Aldrich, C6534) or PBS alone were injected subcutaneously in the dorsal skin of wild-type mice, followed immediately by the intravenous injection of ovalbumin (400 μg/mouse, Sigma-Aldrich). After 4 hours, the skin containing the injection site was removed from euthanized mice. For analysis of edema, the solution of chicken egg albumin contained 0.15% Evans blue dye (Sigma-Aldrich) and measurements were conducted as described (Utomo et al., 2008). For immunostaining of neutrophils, the injected site of skin was excised. 10 μm OCT-embedded, frozen sections were fixed in ice-cold acetone, blocked with Dako protein block solution (DAKO), and incubated with Rat anti-Ly6G Ab (1:100, Biolegend, 127602), Alexa488 conjugated anti-Rat IgG (1:500, Invitrogen, A21208) and DAPI (1:500). Ly6G-positive neutrophils per HPF were counted and averaged.

Acute nephrotoxic serum nephritis—Age and sex-matched mice were given an intravenous injection of 100 μL of nephrotoxic serum (NTS) as described (Tsuboi et al., 2008). Mice were pretreated with 40 μg/mouse i.v. of β-glucan, or dextran 1 hour before NTS injection, and 10 μg/mouse myriocin i.p. every other day for 4 weeks. Mice were euthanized at indicated hours after NTS injection and kidneys were harvested for FACs analysis of neutrophil accumulation as described (Saggu et al., 2018) using PE/Cy7-anti-CD45, APC-anti-Ly6G and FITC-anti-CD11b, PerCp/Cy5.5-anti-Ly6C. The number of neutrophils (CD45+/Ly6G+/CD11b+/Ly6C−) were calculated using counting beads (Invitrogen).

QUANTIFICATION AND STATISTICAL ANALYSIS

Data obtained are presented as the mean ± SEM for all studies except for the evaluation of FcγR affinity for IgG which is mean ± S.D.. Statistical differences were analyzed with unpaired Student’s t test, or one way ANOVA followed by Dunnett’s multiple comparison

test for Gaussian distribution as parametric analysis, and Man-Whitney or Kruskall Wallis test as non-parametric analysis, and P values less than 0.05 were considered significant. P values less than 0.05 were considered significant. Data were analyzed using the JMP 10 software (SAS Institute Inc.) and Prism (GraphPad).

Supplementary Material

Refer to Web version on PubMed Central for supplementary material.

ACKNOWLEDGMENTS

We are grateful to Dr. Akira Shizuo (Department of Host Defense, Research Institute for Microbial Diseases, Osaka University, Suita Osaka, Japan) for providing MyD88/TRIF-deficient mice. This work was supported by the National Institutes of Health grants R01HL065095 (T.N.M.) and U01CA250040 and R01HL132019 (C.Z.), and the National Science Foundation grant DMS-1660504 (C.Z.). This work was also supported (in part) by Immuno Research and Biothera Pharmaceuticals, Inc.

REFERENCES

Abram CL, and Lowell CA (2017). Shp1 function in myeloid cells. J. Leukoc. Biol. 102, 657–675. [PubMed: 28606940]

Abram CL, Roberge GL, Pao LI, Neel BG, and Lowell CA (2013). Distinct roles for neutrophils and dendritic cells in inflammation and autoimmunity in motheaten mice. Immunity 38, 489–501. [PubMed: 23521885]

Anania JC, Trist HM, Palmer CS, Tan PS, Kouskousis BP, Chenoweth AM, Kent SJ, Mackay GA, Hoi A, Koelmeyer R, et al. (2018). The Rare Anaphylaxis-Associated FcγRIIa3 Exhibits Distinct Characteristics From the Canonical FcγRIIa1. Front. Immunol. 9, 1809. [PubMed: 30177930]

Bedja D, Yan W, Lad V, Iocco D, Sivakumar N, Bandaru VVR, and Chatterjee S (2018). Inhibition of glycosphingolipid synthesis reverses skin inflammation and hair loss in ApoE−/− mice fed western diet. Sci. Rep. 8, 11463. [PubMed: 30061606]

Ben Mkaddem S, Hayem G, Jönsson F, Rossato E, Boedec E, Boussetta T, El Benna J, Launay P, Goujon JM, Benhamou M, et al. (2014). Shifting FcγRIIA-ITAM from activation to inhibitory configuration ameliorates arthritis. J. Clin. Invest. 124, 3945–3959. [PubMed: 25061875]

Ben Mkaddem S, Benhamou M, and Monteiro RC (2019). Understanding Fc Receptor Involvement in Inflammatory Diseases: From Mechanisms to New Therapeutic Tools. Front. Immunol. 10, 811. [PubMed: 31057544]

Beppler J, Koehler-Santos P, Pasqualim G, Matte U, Alho CS, Dias FS, Kowalski TW, Velasco IT, Monteiro RC, and Pinheiro da Silva F (2016). Fc Gamma Receptor IIA (CD32A) R131 Polymorphism as a Marker of Genetic Susceptibility to Sepsis. Inflammation 39, 518–525. [PubMed: 26490967]

Bittner S, Bobak N, Hofmann MS, Schuhmann MK, Ruck T, Göbel K, Brück W, Wiendl H, and Meuth SG (2015). Murine K2P5.1 Deficiency Has No Impact on Autoimmune Neuroinflammation due to Compensatory K2P3.1- and KV1.3-Dependent Mechanisms. Int. J. Mol. Sci. 16, 16880–16896. [PubMed: 26213925]

Borzęcka-Solarz K, Dembińska J, Hromada-Judycka A, Traczyk G, Ciesielska A, Ziemlińska E, Świątkowska A, and Kwiatkowska K (2017). Association of Lyn kinase with membrane rafts determines its negative influence on LPS-induced signaling. Mol. Biol. Cell 28, 1147–1159. [PubMed: 28228554]

Bournazos S, Hart SP, Chamberlain LH, Glennie MJ, and Dransfield I (2009). Association of FcgammaRIIa (CD32a) with lipid rafts regulates ligand binding activity. J. Immunol. 182, 8026–8036. [PubMed: 19494328]

Bracke M, Coffer PJ, Lammers JW, and Koenderman L (1998). Analysis of signal transduction pathways regulating cytokine-mediated Fc receptor activation on human eosinophils. J. Immunol. 161, 6768–6774. [PubMed: 9862707]

Bruhns P, and Jönsson F (2015). Mouse and human FcR effector functions. Immunol. Rev. 268, 25–51. [PubMed: 26497511]

Calderwood DA (2004). Integrin activation. J. Cell Sci. 117, 657–666. [PubMed: 14754902]

Carman CV, and Springer TA (2003). Integrin avidity regulation: are changes in affinity and conformation underemphasized? Curr. Opin. Cell Biol. 15, 547–556. [PubMed: 14519389]

Chan VW, Meng F, Soriano P, DeFranco AL, and Lowell CA (1997). Characterization of the B lymphocyte populations in Lyn-deficient mice and the role of Lyn in signal initiation and down-regulation. Immunity 7, 69–81. [PubMed: 9252121]

Chan AS, Jonas AB, Qiu X, Ottoson NR, Walsh RM, Gorden KB, Harrison B, Maimonis PJ, Leonardo SM, Ertelt KE, et al. (2016). Imprime PGG-Mediated Anti-Cancer Immune Activation Requires Immune Complex Formation. PLoS One 11, e0165909. [PubMed: 27812183]

Chen W, Lou J, and Zhu C (2010). Forcing switch from short- to intermediate- and long-lived states of the alphaA domain generates LFA-1/ICAM-1 catch bonds. J. Biol. Chem. 285, 35967–35978. [PubMed: 20819952]

Chesla SE, Selvaraj P, and Zhu C (1998). Measuring two-dimensional receptor-ligand binding kinetics by micropipette. Biophys. J. 75, 1553–1572. [PubMed: 9726957]

Chiani P, Bromuro C, Cassone A, and Torosantucci A (2009). Anti-beta-glucan antibodies in healthy human subjects. Vaccine 27, 513–519. [PubMed: 19041357]

Coxon A, Rieu P, Barkalow FJ, Askari S, Sharpe AH, von Andrian UH, Arnaout MA, and Mayadas TN (1996). A novel role for the beta 2 integrin CD11b/CD18 in neutrophil apoptosis: a homeostatic mechanism in inflammation. Immunity 5, 653–666. [PubMed: 8986723]

Coxon A, Cullere X, Knight S, Sethi S, Wakelin MW, Stavrakis G, Luscinskas FW, and Mayadas TN (2001). Fc gamma RIII mediates neutrophil recruitment to immune complexes. a mechanism for neutrophil accumulation in immune-mediated inflammation. Immunity 14, 693–704. [PubMed: 11420040]

Craggs G, and Kellie S (2001). A functional nuclear localization sequence in the C-terminal domain of SHP-1. J. Biol. Chem. 276, 23719–23725. [PubMed: 11323437]

Crockett-Torabi E, and Fantone JC (1990). Soluble and insoluble immune complexes activate human neutrophil NADPH oxidase by distinct Fc gamma receptor-specific mechanisms. J. Immunol. 145, 3026–3032. [PubMed: 2170530]

Duits AJ, Bootsma H, Derksen RH, Spronk PE, Kater L, Kallenberg CG, Capel PJ, Westerdaal NA, Spierenburg GT, Gmelig-Meyling FH, et al. (1995). Skewed distribution of IgG Fc receptor IIa (CD32) polymorphism is associated with renal disease in systemic lupus erythematosus patients. Arthritis Rheum. 38, 1832–1836. [PubMed: 8849356]

Favier B (2016). Regulation of neutrophil functions through inhibitory receptors: an emerging paradigm in health and disease. Immunol. Rev. 273, 140–155. [PubMed: 27558333]

Filimoniuk A, Blachnio-Zabielska A, Imierska M, Lebensztejn DM, and Daniluk U (2020). Sphingolipid Analysis Indicate Lactosylceramide as a Potential Biomarker of Inflammatory Bowel Disease in Children. Biomolecules 10, 1083.

Florey O, and Haskard DO (2009). Sphingosine 1-phosphate enhances Fc gamma receptor-mediated neutrophil activation and recruitment under flow conditions. J. Immunol. 183, 2330–2336. [PubMed: 19620297]

Florey OJ, Johns M, Esho OO, Mason JC, and Haskard DO (2007). Antiendothelial cell antibodies mediate enhanced leukocyte adhesion to cytokine-activated endothelial cells through a novel mechanism requiring cooperation between FcgammaRIIa and CXCR½. Blood 109, 3881–3889. [PubMed: 17244681]

Folgosa L, Zellner HB, El Shikh ME, and Conrad DH (2013). Disturbed follicular architecture in B cell A disintegrin and metalloproteinase (ADAM)10 knockouts is mediated by compensatory increases in ADAM17 and TNF-α shedding. J. Immunol. 191, 5951–5958. [PubMed: 24227779]

Garg M, Wahid M, and Khan F (2020). Regulation of peripheral and central immunity: Understanding the role of Src homology 2 domain-containing tyrosine phosphatases, SHP-1 & SHP-2. Immunobiology 225, 151847. [PubMed: 31561841]

Goodridge HS, Wolf AJ, and Underhill DM (2009). Beta-glucan recognition by the innate immune system. Immunol. Rev. 230, 38–50. [PubMed: 19594628]

Hakomori S (1981). Glycosphingolipids in cellular interaction, differentiation, and oncogenesis. Annu. Rev. Biochem. 50, 733–764. [PubMed: 7023369]

Hakomori S (2002). Glycosylation defining cancer malignancy: new wine in an old bottle. Proc. Natl. Acad. Sci. USA 99, 10231–10233. [PubMed: 12149519]

Hayes JM, Cosgrave EF, Struwe WB, Wormald M, Davey GP, Jefferis R, and Rudd PM (2014). Glycosylation and Fc receptors. Curr. Top. Microbiol. Immunol. 382, 165–199. [PubMed: 25116100]

Hibbs ML, Tarlinton DM, Armes J, Grail D, Hodgson G, Maglitto R, Stacker SA, and Dunn AR (1995). Multiple defects in the immune system of Lyn-deficient mice, culminating in autoimmune disease. Cell 83, 301–311. [PubMed: 7585947]

Huang J, Zarnitsyna VI, Liu B, Edwards LJ, Jiang N, Evavold BD, and Zhu C (2010). The kinetics of two-dimensional TCR and pMHC interactions determine T-cell responsiveness. Nature 464, 932–936. [PubMed: 20357766]

Ishibashi K, Kurone Y, Motoi M, Miura NN, Adachi Y, Shirasu Y, and Ohno N (2010). The influence of β-glucan on the growth and cell wall architecture of Aspergillus spp. Microbiol. Immunol. 54, 666–672. [PubMed: 21044140]

Iwabuchi K, and Nagaoka I (2002). Lactosylceramide-enriched glycosphingolipid signaling domain mediates superoxide generation from human neutrophils. Blood 100, 1454–1464. [PubMed: 12149231]

Iwabuchi K, Prinetti A, Sonnino S, Mauri L, Kobayashi T, Ishii K, Kaga N, Murayama K, Kurihara H, Nakayama H, et al. (2008). Involvement of very long fatty acid-containing lactosylceramide in lactosylceramide-mediated superoxide generation and migration in neutrophils. Glycoconj. J. 25, 357–374. [PubMed: 18041581]

Iwabuchi K, Nakayama H, Iwahara C, and Takamori K (2010). Significance of glycosphingolipid fatty acid chain length on membrane microdomain-mediated signal transduction. FEBS Lett. 584, 1642–1652. [PubMed: 19852959]

Kerntke C, Nimmerjahn F, and Biburger M (2020). There Is (Scientific) Strength in Numbers: A Comprehensive Quantitation of Fc Gamma Receptor Numbers on Human and Murine Peripheral Blood Leukocytes. Front. Immunol. 11, 118. [PubMed: 32117269]

Khor CC, Davila S, Breunis WB, Lee YC, Shimizu C, Wright VJ, Yeung RS, Tan DE, Sim KS, Wang JJ, et al.; Hong Kong–Shanghai Kawasaki Disease Genetics Consortium; Korean Kawasaki Disease Genetics Consortium; Taiwan Kawasaki Disease Genetics Consortium; International Kawasaki Disease Genetics Consortium; US Kawasaki Disease Genetics Consortium; Blue Mountains Eye Study (2011). Genome-wide association study identifies FCGR2A as a susceptibility locus for Kawasaki disease. Nat. Genet. 43, 1241–1246. [PubMed: 22081228]

Kim MK, Pan XQ, Huang ZY, Hunter S, Hwang PH, Indik ZK, and Schreiber AD (2001). Fc gamma receptors differ in their structural requirements for interaction with the tyrosine kinase Syk in the initial steps of signaling for phagocytosis. Clin. Immunol. 98, 125–132. [PubMed: 11141335]

Koenderman L (2019). Inside-Out Control of Fc-Receptors. Front. Immunol. 10, 544. [PubMed: 30949181]

Koenderman L, Hermans SW, Capel PJ, and van de Winkel JG (1993). Granulocyte-macrophage colony-stimulating factor induces sequential activation and deactivation of binding via a low-affinity IgG Fc receptor, hFc gamma RII, on human eosinophils. Blood 81, 2413–2419. [PubMed: 8481520]

Kong F, García AJ, Mould AP, Humphries MJ, and Zhu C (2009). Demonstration of catch bonds between an integrin and its ligand. J. Cell Biol. 185, 1275–1284. [PubMed: 19564406]

Kovárová M, Tolar P, Arudchandran R, Dráberová L, Rivera J, and Dráber P (2001). Structure-function analysis of Lyn kinase association with lipid rafts and initiation of early signaling events after Fcepsilon receptor I aggregation. Mol. Cell. Biol. 21, 8318–8328. [PubMed: 11713268]

Kumar A, Baycin-Hizal D, Zhang Y, Bowen MA, and Betenbaugh MJ (2015). Cellular traffic cops: the interplay between lipids and proteins regulates vesicular formation, trafficking, and signaling in mammalian cells. Curr. Opin. Biotechnol. 36, 215–221. [PubMed: 26540512]

Kurek K, Wiesiołek-Kurek P, Piotrowska DM, Łukaszuk B, Chabowski A, and Żendzianendzian-Piotrowska M (2014). Inhibition of ceramide de novo synthesis with myriocin affects lipid

metabolism in the liver of rats with streptozotocin-induced type 1 diabetes. BioMed Res. Int. 2014, 980815. [PubMed: 24701589]

Li P, Jiang N, Nagarajan S, Wohlhueter R, Selvaraj P, and Zhu C (2007). Affinity and kinetic analysis of Fcgamma receptor IIIa (CD16a) binding to IgG ligands. J. Biol. Chem. 282, 6210–6221. [PubMed: 17202140]

Limon JJ, Skalski JH, and Underhill DM (2017). Commensal Fungi in Health and Disease. Cell Host Microbe 22, 156–165. [PubMed: 28799901]

Mkaddem SB, Murua A, Flament H, Titeca-Beauport D, Bounaix C, Danelli L, Launay P, Benhamou M, Blank U, Daugas E, et al. (2017). Lyn and Fyn function as molecular switches that control immunoreceptors to direct homeostasis or inflammation. Nat. Commun. 8, 246. [PubMed: 28811476]

Mulder A, Alexander S, Engelfriet CP, von dem Borne AE, and Strominger JL (1981). Characterization, by immunoprecipitation, of myeloidand monocyte-specific antigens present on the human promyelocytic cell line (HL-60) in three stages of differentiation. Proc. Natl. Acad. Sci. USA 78, 5091–5095. [PubMed: 6946457]

Nakayama H, Yoshizaki F, Prinetti A, Sonnino S, Mauri L, Takamori K, Ogawa H, and Iwabuchi K (2008). Lyn-coupled LacCer-enriched lipid rafts are required for CD11b/CD18-mediated neutrophil phagocytosis of non-opsonized microorganisms. J. Leukoc. Biol. 83, 728–741. [PubMed: 18055569]

Nimmerjahn F, and Ravetch JV (2006). Fcgamma receptors: old friends and new family members. Immunity 24, 19–28. [PubMed: 16413920]

Nishi H, Furuhashi K, Cullere X, Saggu G, Miller MJ, Chen Y, Rosetti F, Hamilton SL, Yang L, Pittman SP, et al. (2017). Neutrophil FcγRIIA promotes IgG-mediated glomerular neutrophil capture via Abl/Src kinases. J. Clin. Invest. 127, 3810–3826. [PubMed: 28891817]

Norman MU, Van De Velde NC, Timoshanko JR, Issekutz A, and Hickey MJ (2003). Overlapping roles of endothelial selectins and vascular cell adhesion molecule-1 in immune complex-induced leukocyte recruitment in the cremasteric microvasculature. Am. J. Pathol. 163, 1491–1503. [PubMed: 14507656]

Nowling TK, Mather AR, Thiyagarajan T, Hernández-Corbacho MJ, Powers TW, Jones EE, Snider AJ, Oates JC, Drake RR, and Siskind LJ (2015). Renal glycosphingolipid metabolism is dysfunctional in lupus nephritis. J. Am. Soc. Nephrol. 26, 1402–1413. [PubMed: 25270066]

Ortiz-Stern A, and Rosales C (2003). Cross-talk between Fc receptors and integrins. Immunol. Lett. 90, 137–143. [PubMed: 14687715]

Patel KR, Roberts JT, and Barb AW (2019). Multiple Variables at the Leukocyte Cell Surface Impact Fc g Receptor-Dependent Mechanisms. Front. Immunol. 10, 223. [PubMed: 30837990]

Pereira S, and Lowell C (2003). The Lyn tyrosine kinase negatively regulates neutrophil integrin signaling. J. Immunol. 171, 1319–1327. [PubMed: 12874221]

Pfirsch-Maisonnas S, Aloulou M, Xu T, Claver J, Kanamaru Y, Tiwari M, Launay P, Monteiro RC, and Blank U (2011). Inhibitory ITAM signaling traps activating receptors with the phosphatase SHP-1 to form polarized “in-hibisome” clusters. Sci. Signal. 4, ra24. [PubMed: 21505186]

Pike LJ (2004). Lipid rafts: heterogeneity on the high seas. Biochem. J. 378, 281–292. [PubMed: 14662007]

Poulain D, and Jouault T (2004). Candida albicans cell wall glycans, host receptors and responses: elements for a decisive crosstalk. Curr. Opin. Microbiol. 7, 342–349. [PubMed: 15358252]

Radstake TR, Petit E, Pierlot C, van de Putte LB, Cornelis F, and Barrera P (2003). Role of Fcgamma receptors IIA, IIIA, and IIIB in susceptibility to rheumatoid arthritis. J. Rheumatol. 30, 926–933. [PubMed: 12734884]

Rahar S, Swami G, Nagpal N, Nagpal MA, and Singh GS (2011). Preparation, characterization, and biological properties of β-glucans. J. Adv. Pharm. Technol. Res. 2, 94–103. [PubMed: 22171300]

Renaudineau Y, Dugué C, Dueymes M, and Youinou P (2002). Antiendothelial cell antibodies in systemic lupus erythematosus. Autoimmun. Rev. 1, 365–372. [PubMed: 12848993]

Roeder A, Kirschning CJ, Rupec RA, Schaller M, Weindl G, and Korting HC (2004). Toll-like receptors as key mediators in innate antifungal immunity. Med. Mycol. 42, 485–498. [PubMed: 15682636]

Rosetti F, Chen Y, Sen M, Thayer E, Azcutia V, Herter JM, Luscinskas FW, Cullere X, Zhu C, and Mayadas TN (2015). A Lupus-Associated Mac-1 Variant Has Defects in Integrin Allostery and Interaction with Ligands under Force. Cell Rep. 10, 1655–1664. [PubMed: 25772353]

Rossi GM, Bonatti F, Adorni A, Alberici F, Bodria M, Bonanni A, Ghiggeri GM, Martorana D, and Vaglio A (2018). FCGR2A single nucleotide polymorphism confers susceptibility to childhood-onset idiopathic nephrotic syndrome. Immunol. Lett. 193, 11–13. [PubMed: 29155175]

Sadras V, Petri MA, Jones SR, Peterlin BL, and Chatterjee S (2020). Glycosphingolipid-associated β −1,4 galactosyltransferase is elevated in patients with systemic lupus erythematosus. Lupus Sci. Med. 7, e00368.

Saggu G, Okubo K, Chen Y, Vattepu R, Tsuboi N, Rosetti F, Cullere X, Washburn N, Tahir S, Rosado AM, et al. (2018). Cis interaction between sialylated FcγRIIA and the αI-domain of Mac-1 limits antibody-mediated neutrophil recruitment. Nat. Commun. 9, 5058. [PubMed: 30498196]

Saijo K, Schmedt C, Su IH, Karasuyama H, Lowell CA, Reth M, Adachi T, Patke A, Santana A, and Tarakhovsky A (2003). Essential role of Src-family protein tyrosine kinases in NF-kappaB activation during B cell development. Nat. Immunol. 4, 274–279. [PubMed: 12563261]

Sato T, Iwabuchi K, Nagaoka I, Adachi Y, Ohno N, Tamura H, Seyama K, Fukuchi Y, Nakayama H, Yoshizaki F, et al. (2006). Induction of human neutrophil chemotaxis by Candida albicans-derived beta-1,6-long glycoside side-chain-branched beta-glucan. J. Leukoc. Biol. 80, 204–211. [PubMed: 16670126]

Scapini P, Lapinet-Vera JA, Gasperini S, Calzetti F, Bazzoni F, and Cassatella MA (2000). The neutrophil as a cellular source of chemokines. Immunol. Rev. 177, 195–203. [PubMed: 11138776]

Scapini P, Pereira S, Zhang H, and Lowell CA (2009). Multiple roles of Lyn kinase in myeloid cell signaling and function. Immunol. Rev. 228, 23–40. [PubMed: 19290919]

Segal NH, Gada P, Senzer N, Gargano MA, Patchen ML, and Saltz LB (2016). A Phase II Efficacy and Safety, Open-Label, Multicenter Study of Imprime PGG Injection in Combination With Cetuximab in Patients With Stage IV KRAS-Mutant Colorectal Cancer. Clin. Colorectal Cancer 15, 222–227. [PubMed: 26975418]

Seumois G, Fillet M, Gillet L, Faccinetto C, Desmet C, Franç ois C, Dewals B, Oury C, Vanderplasschen A, Lekeux P, and Bureau F (2007). De novo C16- and C24-ceramide generation contributes to spontaneous neutrophil apoptosis. J. Leukoc. Biol. 81, 1477–1486. [PubMed: 17329567]

Sondermann P, Kaiser J, and Jacob U (2001). Molecular basis for immune complex recognition: a comparison of Fc-receptor structures. J. Mol. Biol. 309, 737–749. [PubMed: 11397093]

Springer TA, and Dustin ML (2012). Integrin inside-out signaling and the immunological synapse. Curr Opin Cell Biol 24, 107–115. [PubMed: 22129583]

Stewart M, and Hogg N (1996). Regulation of leukocyte integrin function: affinity vs. avidity. J. Cell. Biochem. 61, 554–561. [PubMed: 8806078]

Stokol T, O'Donnell P, Xiao L, Knight S, Stavrakis G, Botto M, von Andrian UH, and Mayadas TN (2004). C1q governs deposition of circulating immune complexes and leukocyte Fcgamma receptors mediate subsequent neutrophil recruitment. J. Exp. Med. 200, 835–846. [PubMed: 15466618]

Sud M, Fahy E, Cotter D, Brown A, Dennis EA, Glass CK, Merrill AH Jr., Murphy RC, Raetz CR, Russell DW, and Subramaniam S (2007). LMSD: LIPID MAPS structure database. Nucleic Acids Res. 35, D527–D532. [PubMed: 17098933]

Sylvestre DL, and Ravetch JV (1994). Fc receptors initiate the Arthus reaction: redefining the inflammatory cascade. Science 265, 1095–1098. [PubMed: 8066448]

Sylvestre DL, and Ravetch JV (1996). A dominant role for mast cell Fc receptors in the Arthus reaction. Immunity 5, 387–390. [PubMed: 8885871]

Tang T, Rosenkranz A, Assmann KJ, Goodman MJ, Gutierrez-Ramos JC, Carroll MC, Cotran RS, and Mayadas TN (1997). A role for Mac-1 (CDIIb/CD18) in immune complex-stimulated neutrophil function in vivo: Mac-1 deficiency abrogates sustained Fcgamma receptor-dependent neutrophil adhesion and complement-dependent proteinuria in acute glomerulonephritis. J. Exp. Med. 186, 1853–1863. [PubMed: 9382884]

Thomas M, Sadjadian P, Kollmeier J, Lowe J, Mattson P, Trout JR, Gargano M, Patchen ML, Walsh R, Beliveau M, et al. (2017). A randomized, open-label, multicenter, phase II study evaluating the efficacy and safety of BTH1677 (1,3–1,6 beta glucan; Imprime PGG) in combination with cetuximab and chemotherapy in patients with advanced non-small cell lung cancer. Invest. New Drugs 35, 345–358. [PubMed: 28303530]

Tsuboi N, Asano K, Lauterbach M, and Mayadas TN (2008). Human neutrophil Fcgamma receptors initiate and play specialized nonredundant roles in antibody-mediated inflammatory diseases. Immunity 28, 833–846. [PubMed: 18538590]

Tsuboi N, Ernandez T, Li X, Nishi H, Cullere X, Mekala D, Hazen M, Köhl J, Lee DM, and Mayadas TN (2011). Regulation of human neutrophil Fcγ receptor IIa by C5a receptor promotes inflammatory arthritis in mice. Arthritis Rheum. 63, 467–478. [PubMed: 21280001]

Utomo A, Hirahashi J, Mekala D, Asano K, Glogauer M, Cullere X, and Mayadas TN (2008). Requirement for Vav proteins in post-recruitment neutrophil cytotoxicity in IgG but not complement C3-dependent injury. J. Immunol. 180, 6279–6287. [PubMed: 18424751]

Wakshull E, Brunke-Reese D, Lindermuth J, Fisette L, Nathans RS, Crowley JJ, Tufts JC, Zimmerman J, Mackin W, and Adams DS (1999). PGG-glucan, a soluble beta-(1,3)-glucan, enhances the oxidative burst response, microbicidal activity, and activates an NF-kappa B-like factor in human PMN: evidence for a glycosphingolipid beta-(1,3)-glucan receptor. Immunopharmacology 41, 89–107. [PubMed: 10102791]

Walls SM, Cammarato A, Chatfield DA, Ocorr K, Harris GL, and Bodmer R (2018). Ceramide-Protein Interactions Modulate Ceramide-Associated Lipotoxic Cardiomyopathy. Cell Rep. 22, 2702–2715. [PubMed: 29514098]

Wang Y, and Jönsson F (2019). Expression, Role, and Regulation of Neutrophil Fcγ Receptors. Front. Immunol. 10, 1958. [PubMed: 31507592]

Xia SL, Lin DP, Lin QR, Sun L, Wang XQ, Hong WJ, Lin ZJ, Du CC, and Jiang Y (2018). A Case-Control Study on Association of Ulcerative Colitis with FCGR2A Gene Polymorphisms in Chinese Patients. Genet. Test. Mol. Biomarkers 22, 607–614. [PubMed: 30260678]

Xiong Y, Cao C, Makarova A, Hyman B, and Zhang L (2006). Mac-1 promotes FcgammaRIIA-dependent cell spreading and migration on immune complexes. Biochemistry 45, 8721–8731. [PubMed: 16846215]

Yago T, Lou J, Wu T, Yang J, Miner JJ, Coburn L, López JA, Cruz MA, Dong JF, McIntire LV, et al. (2008). Platelet glycoprotein Ibalpha forms catch bonds with human WT vWF but not with type 2B von Willebrand disease vWF. J. Clin. Invest. 118, 3195–3207. [PubMed: 18725999]

Yamamoto M, Sato S, Hemmi H, Uematsu S, Hoshino K, Kaisho T, Takeuchi O, Takeda K, and Akira S (2003). TRAM is specifically involved in the Toll-like receptor 4-mediated MyD88-independent signaling pathway. Nat. Immunol. 4, 1144–1150. [PubMed: 14556004]

Yan J, Vetvicka V, Xia Y, Coxon A, Carroll MC, Mayadas TN, and Ross GD (1999). Beta-glucan, a “specific” biologic response modifier that uses antibodies to target tumors for cytotoxic recognition by leukocyte complement receptor type 3 (CD11b/CD18). J. Immunol. 163, 3045–3052. [PubMed: 10477568]

Zarnitsyna VI, and Zhu C (2011). Adhesion frequency assay for in situ kinetics analysis of cross-junctional molecular interactions at the cell-cell interface. J. Vis. Exp, e3519. [PubMed: 22083316]

Zhou D, Collins CA, Wu P, and Brown EJ (2010). Protein tyrosine phosphatase SHP-1 positively regulates TLR-induced IL-12p40 production in macrophages through inhibition of phosphatidylinositol 3-kinase. J. Leukoc. Biol. 87, 845–855. [PubMed: 20145200]

Zhu C, Yago T, Lou J, Zarnitsyna VI, and McEver RP (2008). Mechanisms for flow-enhanced cell adhesion. Ann. Biomed. Eng. 36, 604–621. [PubMed: 18299992]

Zimmerman JW, Lindermuth J, Fish PA, Palace GP, Stevenson TT, and DeMong DE (1998). A novel carbohydrate-glycosphingolipid interaction between a beta-(1–3)-glucan immunomodulator, PGG-glucan, and lactosylceramide of human leukocytes. J. Biol. Chem. 273, 22014–22020. [PubMed: 9705343]

Highlights

- Neutrophil FcγRIIA binding to IgG under flow is reduced by a fungal soluble β-glucan
- Binding of β-glucan to the glycosphingolipid lactosylceramide reduces FcγRIIA affinity
- β-glucan-lactosylceramide induces “inside-out” signals to reduce FcγRIIA affinity
- β-glucan reduces IgG-glomerular neutrophil influx that is reversed by Lyn deletion

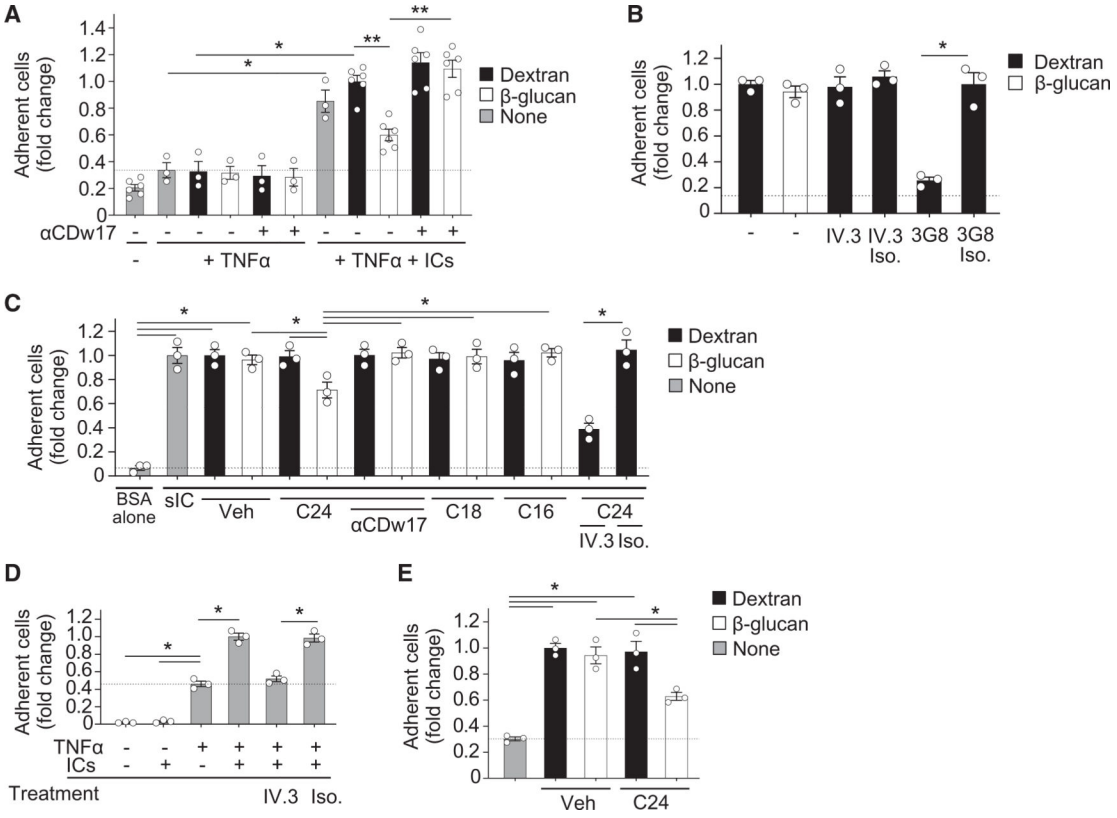

Figure 1. β-glucan inhibits FcγRIIA-mediated cell binding to immune complexes (ICs) under flow by a LacCer-dependent mechanism

(A) Human peripheral blood neutrophils (hPMNs) were perfused at 1.0 dynes/cm^2 over TNF-α-activated human dermal microvascular endothelial cells (HDMECs) with or without anti-endoglin (IC) coating. After 1 min of continuous perfusion, the number of adherent cells was counted in four random fields. Human neutrophils were untreated (none) or pretreated with 1,3–1,6 beta(β)-glucan (β-glucan) or dextran (control for β-glucan) and anti-lactosylceramide (LacCer) antibody (anti-CDw17 Ab) as indicated prior to their perfusion.

(B) hPMNs were perfused across coverslip-immobilized, preformed soluble ICs (sICs; BSA-anti-BSA) at 1.0 dynes/cm^2. Cells were treated with β-glucan or dextran, functional blocking antibody to FcγRIIA (IV.3) or FcγRIIIB (3G8), or their respective isotype controls prior to their perfusion.

(C) DMF-differentiated HL60 cells transduced with FcγRIIA (HL60–2A) were perfused across coverslip-immobilized BSA-anti-BSA sICs or BSA alone at 0.5 dynes/cm^2. HL60–2A cells were untreated (none) or pretreated with LacCer C24, C18, C16, vehicle and β-glucan or dextran, or anti-LacCer Ab (αCDw17), functional blocking anti-CD32 Ab (IV.3) or isotype control (Iso), as indicated; and the number of adherent cells was analyzed as in (A).

(D and E) DMF-differentiated HL60–2A cells were pretreated with IV.3 or isotype control (D) or with LacCer C24, vehicle, and β-glucan or dextran (E) and perfused across TNF-α-activated HDMECs coated with ICs and analyzed as in (A).

Bar graphs represent fold change compared to TNF-α + ICs + dextran for (A), dextran for (B), HL60–2A + vehicle +dextran for (C) and (E), and TNF-α + ICs for (D). Dotted line

represents the value of TNF-α-activated HDMECs for (A), (D), and (E) and BSA alone for (B) and (C). Data are average ± SEM, and individual values are plotted. *$p < 0.05$, **$p < 0.01$ using the Kruskal-Wallis test.

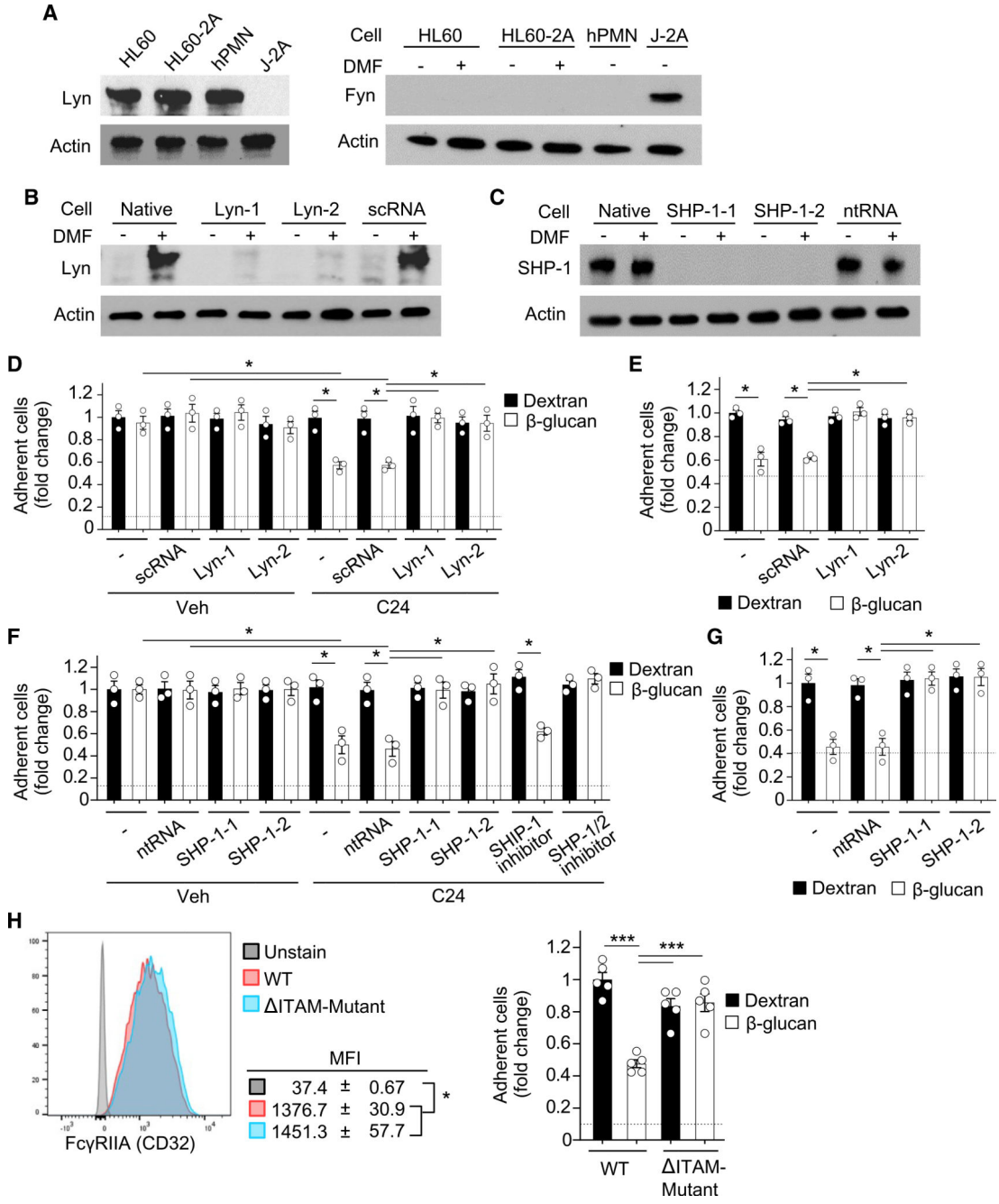

Figure 2. β-glucan-mediated inhibition of FcγRIIA-dependent cell binding to immune complexes requires Lyn, SHP-1, and the ITAM of FcγRIIA

(A) Lysates from DMF-differentiated or undifferentiated HL60 cells or transduced with FcγRIIA (HL60–2A) and hPMN and Jurkat cells transduced with FcγRIIA (J2A) were subjected to western blot analysis by using antibodies to Lyn (left), Fyn (right), or actin (loading control).

(B and C) HL60–2A parent cell line (native) or HL60–2A with Lyn shRNA clone 1 or 2 or scrambled shRNA control (Lyn-1, Lyn-2, and scRNA) (B) or with SHP-1 shRNA clone 1 or 2 or non-target shRNA control (SHP-1–1, SHP-1–2, and ntRNA) (C) were left untreated (−)

or DMF treated (+) to induce differentiation. Cell lysates were evaluated for Lyn and SHP-1 and actin as a loading control. Representative images of 1 of 3 experiments are shown.
(D and E) DMF-differentiated HL60–2A (−), Lyn-1, Lyn-2, or scRNA were treated with LacCer C24, vehicle, and β-glucan or dextran and perfused across immobilized BSA-anti-BSA (D) or TNF-α-activated HDMECs coated with anti-endoglin (E) and analyzed as in Figure 1.
(F and G) DMF-differentiated HL60–2A parent cell line (−), SHP-1–1, SHP-1–2, or ntRNA treated with SHIP-1 inhibitor, SHP-1/2 inhibitor, and indicated drugs were perfused across immobilized BSA-anti-BSA (F) or TNF-α-activated HDMECs coated with anti-endoglin IC (G) and evaluated as in Figure 1.
(H) Surface expression level of FcγRIIA in DMF-differentiated HL60 expressing wild-type FcγRIIA (WT) or FcγRIIA ΔITAM mutant was evaluated by fluorescence-activated cell sorting (FACS) (left). n = 3. Cells were treated with LacCer C24 and β-glucan or dextran and perfused across immobilized BSA-anti-BSA (right).
Bar graphs represent fold change compared to (−) + vehicle + dextran for (D) and (F), (−) + dextran for (E) and (G), and HL60–2A + dextran for (H). Dotted lines represent the value of BSA alone for (D, (F), and (H) and TNF-α-activated HDMECs for (E) and (G). Data are average ± SEM, and individual values are plotted. *$p < 0.05$, ***$p < 0.001$ using the one-way ANOVA followed by Dunnett's multiple comparison test for (H) (right) or Kruskal-Wallis test for (D)–(H) (left).

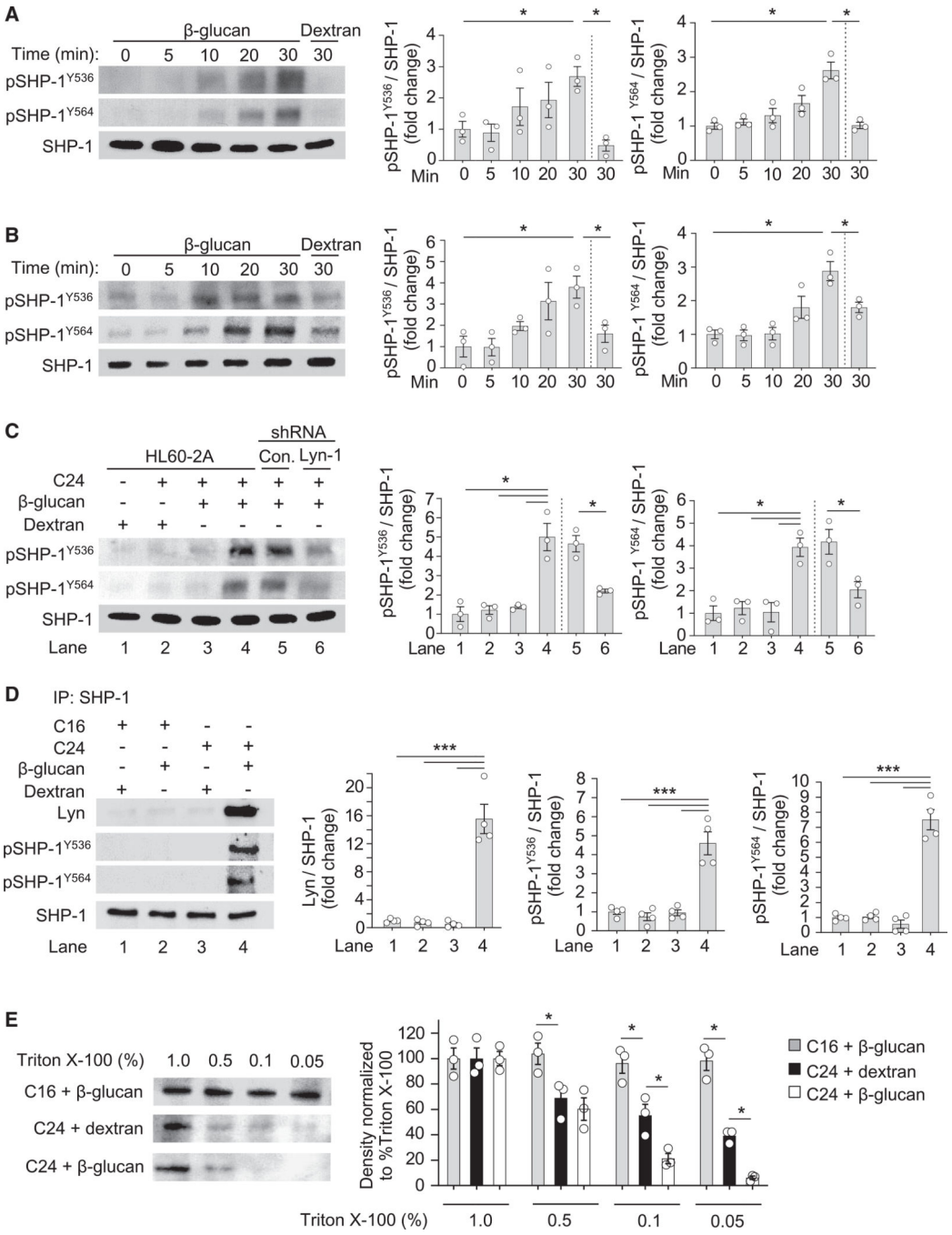

Figure 3. β-glucan mediates pSHP-1^{Y536} and pSHP-1^{Y564} phosphorylation that is dependent on Lyn

(A) Lysates from DMF-differentiated HL60 expressing FcγRIIA (HL60–2A) treated with LacCer C24 and β-glucan for indicated times in min or dextran for 30 mins were subjected to western blot analysis using antibody to pSHP-1^{Y536}, pSHP-1^{Y564}, and total SHP-1 (loading control). Representative blot and quantitation normalized to total SHP-1 are shown. (B) Lysates from human neutrophils which were treated as in (A) were subjected to western blot analysis.

(C) Lysates from DMF-differentiated HL60–2A, Lyn shRNA (Lyn-1), and scRNA control (Con.) cells, which were treated as in (A) for 30 mins and subjected to western blot analysis.
(D) Lysates immunoprecipitated with SHP-1 from differentiated HL60–2A treated with C16, C24, dextran, or β-glucan were subjected to western blot analysis. Representative blot and quantitation normalized to total SHP-1 are shown.
(E) Differentiated HL60–2A cells were treated as indicated, and lysates were extracted with 0.05, 0.1, 0.5, or 1.0% Triton X-100 and subjected to western blot analysis using anti-Lyn antibody. Densitometric analysis was performed and normalized to 1% Triton X-100 as 100%.
Bar graphs represent fold change compared to 0 min for (A) and (B) and lane 1 for (C) and (D). Data are average ± SEM, and individual values are plotted. *$p < 0.05$, ***$p < 0.001$ using the one-way ANOVA followed by Dunnett's multiple comparison test for (D) or Kruskal-Wallis test for (A)–(C) and (E).

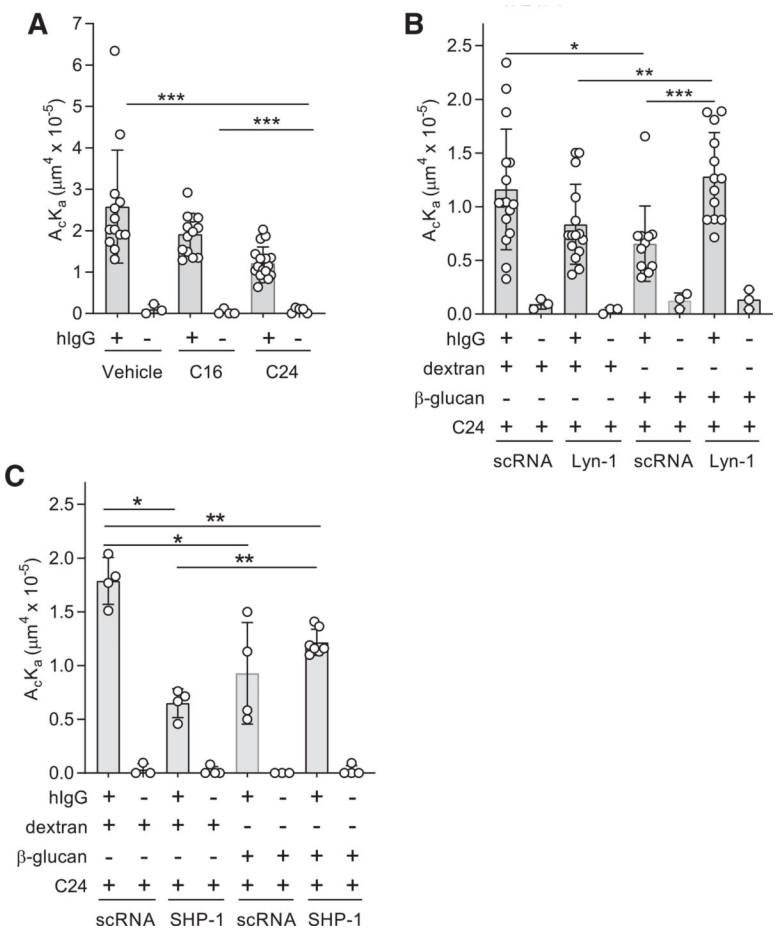

Figure 4. β-glucan decreases FcγRIIA effective 2D affinity for hIgG in a LacCer C24- and Lyn- and SHP-1-dependent manner

(A) DMF-differentiated HL60 cells expressing FcγRIIA (HL60–2A) treated with β-glucan exhibited decreased affinity for hIgG-coated RBCs in the presence of LacCer C24 compared with LacCer C16 or vehicle. Non-specific binding as measured with RBCs without hIgG was negligible.

(B) Lyn knockdown HL60–2A cells (Lyn-1) showed increased affinity for hIgG-coated RBCs compared to scRNA control in the presence of β-glucan but not in dextran.

(C) SHP-1 knockdown HL60–2A cells showed similar results as Lyn-1 knockdown cells, with the addition of β-glucan leading to increased 2D affinity of knockdown cells for IgG. Conversely, there was a significant drop in affinity upon SHP-1 knockdown in the presence of dextran control.

All measurements in (B) and (C) were in the presence of LacCer C24. Non-specific binding controls without hIgG are shown. A_cK_a values represent ligand-receptor density normalized adhesion frequencies. Data are average ± SD, and individual values are plotted. *$p < 0.05$, **$p < 0.01$, ***$p < 0.001$ using an unpaired Student's t test.

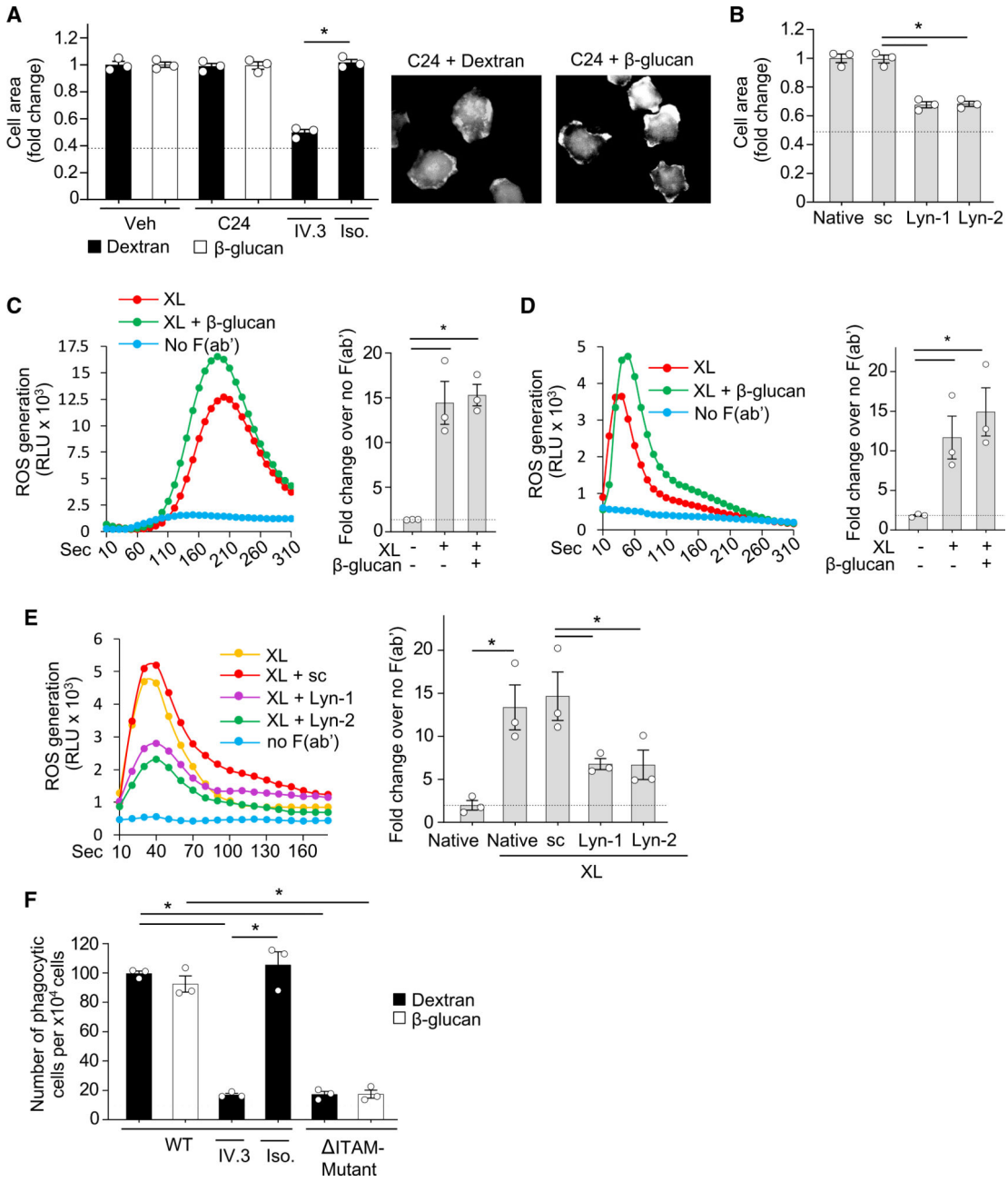

Figure 5. β-glucan has no effect on FcγRIIA-induced cell spreading, reactive oxygen species (ROS) generation, or phagocytosis

(A) DMF-differentiated HL60 cells expressing FcγRIIA (HL60–2A) were treated with vehicle or C24, dextran or β-glucan, and isotype or functional blocking FcγRIIA antibody (IV.3) as indicated. Cells were seeded on immobilized BSA-anti-BSA under static conditions and stained with phalloidin. The area of spread cells and representative images are shown.

(B) DMF-differentiated HL60, HL60–2A with scRNA, Lyn shRNA-1 (Lyn-1), or Lyn shRNA-2 (Lyn-2) were evaluated as in (A).

(C–E) Human neutrophils (C), HL60–2A cells (D) pretreated with C24 and β-glucan, or HL60–2A cells with indicated shRNAs (E) were treated with IV.3 followed with luminol and anti-mouse F(ab') to induce cross-linking (XL), and ROS generation (relative light units [RLUs]) was monitored over time. Representative plots (left) and the peak level of ROS (right) for each condition that was normalized to the average of the F(ab') untreated control are shown.

(F) HL60 cells expressing wild-type FcγRIIA (WT) or FcγRIIA ΔITAM mutant were treated with LacCer C24 and β-glucan, dextran, IV.3, or isotype control as indicated and incubated with IgG-opsonized fluorescein isothiocyanate (FITC)-latex beads. Phagocytic index (percentage of FITC-positive cells over total cells) analyzed by FACS is shown.

Bar graphs represent fold change compared to vehicle + dextran for (A), native for (B), and WT + dextran for (F). Dotted line represents the value of untreated HL60 for (A), (B), and (F) and no F(ab') control for (C), (D), and (E). Data are average ± SEM, and individual values are plotted. *$p < 0.05$ using the Kruskal-Wallis test.

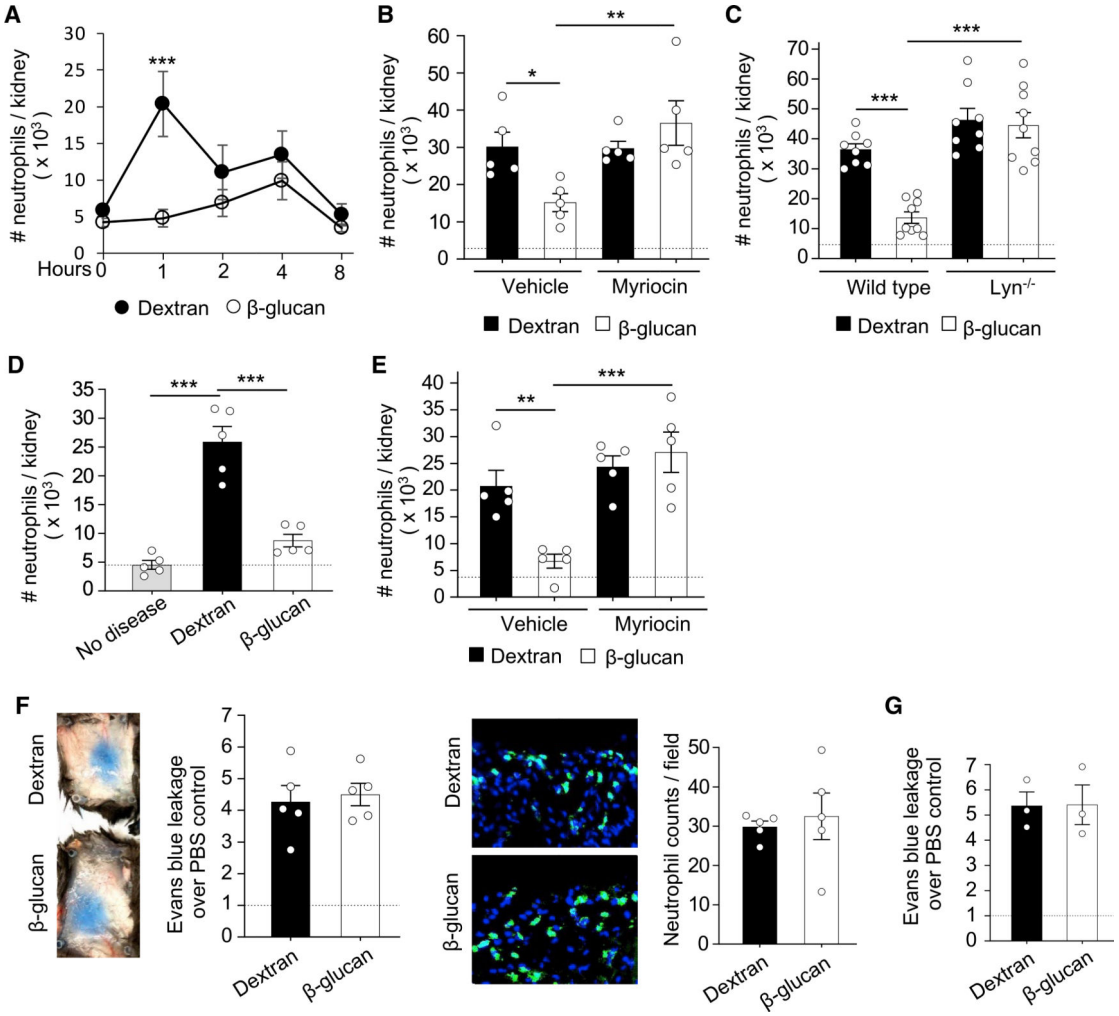

Figure 6. β-glucan inhibits renal neutrophil recruitment after nephrotoxic serum nephritis but has no effect on neutrophil infiltration and tissue injury in the reverse Arthus reaction.

(A) Wild-type mice were given β-glucan (open circle) or dextran (closed circle) intravenously (i.v.) 1 h before i.v. injection of nephrotoxic serum (NTS). At indicated times after NTS injection, kidneys were harvested and infiltrating renal neutrophil accumulation per kidney was quantitated by FACS analysis.

(B) Wild-type mice were pretreated with myriocin for 4 weeks, treated with β-glucan or dextran, and subjected to NTS injection. After 1 h of NTS injection, kidneys were harvested and the number of neutrophils per kidney was quantitated.

(C) Wild-type or Lyn knocked out mice were given β-glucan or dextran, injected with NTS, and evaluated as in (A).

(D) Mice expressing human FcγRIIA selectively on neutrophils lacking their endogenous FcγRs (RIIAtg/$\gamma^{-/-}$) were given β-glucan or dextran and evaluated as in (A).

(E) RIIAtg/$\gamma^{-/-}$ mice were treated with myriocin as indicated and evaluated as in (B).

(F) The reverse passive Arthus (RPA) reaction was induced in wild-type mice by the subcutaneous administration of anti-ovalbumin (OVA) antibody or PBS(control) and the intravenous injection of OVA with Evans blue dye. Representative pictures of skins harvested 4 h after anti-OVA injection are shown (left). Extravasated Evans blue in the skin

was quantitated by blue dye extraction in DMF and measurement of absorbance at optical density 595 (OD595) (middle left). Neutrophil infiltration into the skin after induction of the RPA reaction was evaluated by Ly6G (green) and 4',6-diamidino-2-phenylindole (DAPI, blue) staining (middle right), and the number of neutrophils was quantitated (right).
(G) The RPA reaction was induced in RIIAtg/$\gamma^{-/-}$ mice, and extravasated Evans blue in the skin was quantitated as in (F).
Dotted line represents the value of wild-type mice for (B) and (C) or RIIAtg/$\gamma^{-/-}$ mice for (D) and (E), which did not receive any drugs including NTS (no disease), and PBS control for (F) and (G). Data in bar graphs are average ± SEM and individual values are plotted. *$p < 0.05$, **$p < 0.001$, ***$p < 0.001$ using one-way ANOVA followed by Dunnett's multiple comparison test for (A)–(F) or Mann Whitney U test for (G).

KEY RESOURCES TABLE

REAGENT or RESOURCE	SOURCE	IDENTIFIER
Antibodies		
anti-CDw17 antibody	MyBioSource	Cat# MBS439045
anti-human CD16 Antibody	Biolegend	Cat# 302001 RRID:AB_314201
Purified Mouse IgG1, κ Isotype Control	BD bioscience	Cat# 557273 RRID:AB_396613
anti-human CD32 Antibody	STEMCELL	Cat# 60012 RRID:AB_2722545
Purified Mouse IgG2b	Invitrogen	Cat# MG2B00
anti-human CD105 Ab	Biolegend	Cat# 323202 RRID:AB_755954
anti-BSA antibody	Sigma-Aldrich	Cat# B7276 RRID:AB_258608
anti-mouse antibody	Dako	Cat# Z0259 RRID:AB_2532147
anti-Ly6G antibody	Biolegend	Cat# 127602 RRID:AB_1089180
FITC-anti-CD16	BD bioscience	Cat# 555406 RRID:AB_395806
FITC-anti-CD32	BD bioscience	Cat# 555448 RRID:AB_395841
PE/Cy7-anti-CD11b	Biolegend	Cat# 101216 RRID:AB_312799
FITC-anti-CD11b	Biolegend	Cat# 101206 RRID:AB_312789
PE/Cy7-anti-CD45	Biolegend	Cat# 103114 RRID:AB_312979
APC-anti-Ly6G	Biolegend	Cat# 127614 RRID:AB_2227348
PerCP/Cy5.5-anti-Ly6C	Biolegend	Cat# 128012 RRID:AB_1659241
HRP-anti-Lyn	Cell signaling	Cat# 2796T RRID:AB_2138391
HRP-anti-Fyn	Cell signaling	Cat# 4023T RRID:AB_10698604
anti-pSHP-1 Y536	ECM Bioscience	Cat# SP1571 RRID:AB_2173700
anti-pSHP-1 Y564	Cell signaling	Cat# 8849 RRID:AB_11141050
anti-SHP-1	LifeSpan BioSciences	Cat# LS-C358839
anti-actin	Sigma-Aldrich	Cat# A5316 RRID:AB_476743
Mouse anti-SHP-1	Santa Cruz	Cat# sc7289 RRID:AB_628251
goat anti-mouse F(ab')	Jackson ImmunoResearch	Cat# 115-006-006 RRID:AB_2338467
anti-chicken egg albumin IgG	Sigma-Aldrich	Cat# C6534 RRID:AB_258953
Human IgG Isotype Control [Biotin]	Novus Biologicals	Cat# NBP1-96855
Goat F(ab')2 polyclonal Secondary Antibody to Human IgG - Fc (PE)	Abcam	Cat# ab98596, RRID:AB_10673825
Mouse Anti-CD32 Monoclonal Antibody, Phycoerythrin Conjugated	BD bioscience	Cat# 550586, RRID:AB_393766
Mouse IgG2b, k antibody,	BD bioscience	Cat# 555743, RRID:AB_396086
Chemicals, peptides, and recombinant proteins		
Recombinant Human TNF-α	Peprotech	Cat# 300-01A
K118 (SHIP1 Inhibitor)	Echelon	Cat# B-0344
NSC 87877 (SHP-1/2 inhibitor)	Tocris	Cat# 2613
C24:1 Lactosyl(β) Ceramide (d18:1/24:1)	Avanti	Cat# 860597
C24 Lactosyl(β) Ceramide (d18:1/24:0)	Avanti	Cat# 860577

REAGENT or RESOURCE	SOURCE	IDENTIFIER
C18 Lactosyl(β) Ceramide (d18:1/18:0)	Avanti	Cat# 860598
C16 Lactosyl(β) Ceramide (d18:1/16:0)	Avanti	Cat# 860576
Myriocin	Cayman Chemical	Cat# 63150
Critical commercial assays		
Phagocytosis Assay Kit (IgG FITC)	Cayman Chemical	Cat# 500290
Dynabeads Protein G for Immunoprecipitation	Invitrogen	Cat# 10003D
Quantibrite PE Beads 10 Tubes antibody	BD bioscience	Cat# 340495, RRID:AB_2868736
Experimental models: Cell lines		
HL-60	ATCC	Cat# CCL-240
Human Dermal Microvascular Endothelial Cells	Lonza	Cat# CC-2543
Wild type mice (C57/BL6j)	This paper	N/A
RIIAtg/$\gamma^{-/-}$ mice	This paper	N/A
Mac-1 knock-out mice	This paper	N/A
Dectin-1 knock-out mice	The Jackson Laboratory	Cat# Clec7a/J
MyD88/TRIF knock-out mice	Yamamoto et al., 2003	N/A
Lyn knock-out mice	Pereira and Lowell, 2003	N/A
Software and algorithms		
GraphPad Prism9	GraphPad Software	https://www.graphpad.com/
Photoshop CC	Adobe Software	https://www.adobe.com/products/photoshop.html
FlowJo (Version10.4.2)	FlowJo LLC	https://www.flowjo.com/
JMP 10 software	SAS Institute Inc	https://www.jmp.com/en_us/home.geo.html